

MASTER THESIS

TARGETING INTEGRINS FOR SELF-STIMULATING CELLS WITH BMP-7 BY USING BISPECIFIC VHHS

Anne Grobbink

Developmental BioEngineering
Prof. dr. Marcel Karperien

EXAMINATION COMMITTEE
Prof. dr. Marcel Karperien
Dr. Ruchi Bansal
Supervisor: MSc Michelle Koerselman

January 28, 2021

Abstract

Osteoarthritis (OA) is one of the most common chronic health conditions and causes major disability worldwide. There is an urgent need to develop a minimally invasive, disease-modifying treatment for the regeneration of cartilage. To date, BMP-7 has proven to be one of the most effective growth factors in enhancing the anabolic activity of chondrocytes. In this proof of principle study, bispecific VHHs were used to target Integrin β 1 (ITGB1) and BMP-7 simultaneously to enable controlled BMP-7 delivery *in vitro* as a possible therapy for OA. First, the binding affinity of the two bispecific VHH (G7-FSH-14F8 and G7-WHR-3C9) was characterized with surface plasmon resonance imaging (SPRi). To localize and confirm binding and dual binding, immunofluorescence assays were performed. Pathway activation after BMP-7 stimulation in presence or absence of VHHs was assessed with luciferase, qPCR, and western blot assays. SPRi showed a high binding affinity of both bispecific VHHs for ITGB1 and BMP-7. Immunofluorescent assays showed binding of FSH-14F8 and Bi14F8 towards ITGB1 located at the focal adhesions and resulted in reduced binding of cells, whereas WHR-3C9 and Bi3C9 showed less impact on cell stretching and binding towards ITGB1 showed a diffuse signal over the entire cell surface. Furthermore, luciferase and qPCR assays resulted in higher expression levels after stimulation with Bi3C9, compared to Bi14F8. In conclusion, it was shown that both VHHs can be exploited for long term BMP-7 delivery. This study suggests that Bi3C9 showed preferable characteristics and should be used in future *in vitro* experiments. To target chondrocytes *in vivo*, bispecific VHHs targeting BMP-7 and a tissue-specific protein need to be developed. This thesis has clearly shown that bispecific VHHs can be used for targeted delivery of BMP-7 *in vitro* and shows great promise for disease-modifying treatments for the regeneration of cartilage.

Samenvatting

Artrose is een van de meest voorkomende chronische aandoeningen waar wereldwijd miljoenen patiënten aan lijden. Er is een dringende behoefte aan geneesmiddelen die het ziekteverloop kunnen beïnvloeden, zodat kraakbeen geregenereerd kan worden. Tot op heden is BMP-7 de meest effectieve groeifactor voor het verhogen van de anabole activiteit van chondrocyten. In deze 'proof of principle' studie worden bispecifieke VHHs gebruikt om Integrine $\beta 1$ (ITGB1) en BMP-7 tegelijkertijd te binden voor gecontroleerde afgifte van BMP-7 *in vitro*, als mogelijke therapie voor artrose. De affiniteit van de bispecifieke VHHs (G7-FSH-14F8 en G7-WHR-3C9) werd als eerste bepaald met surface plasmon resonance imaging (SPRi). Om de binding van de VHHs te lokaliseren werden immunofluorescentie experimenten uitgevoerd. Signaaltransductie na BMP-7 stimulatie in aan- of afwezigheid van VHHs werd beoordeeld met luciferase, qPCR en western blot experimenten. Het SPRi experiment liet voor beide bispecifieke VHHs een hoge affiniteit zien voor ITGB1 en BMP-7. Immunofluorescentie experimenten lieten binding van FSH-14F8 en Bi14F8 in de 'focal adhesions' zien met als resultaat een verminderde binding van cellen. Deze impact op hechting van de cellen was niet zichtbaar bij gebruik van WHR-3C9 en Bi3C9 en de binding van deze VHHs aan ITGB1 liet een diffuus signaal over het gehele celmembraan zien. Bovendien liet Bi3C9 in vergelijking met Bi14F8 een verhoogde expressie zien, na stimulatie in de luciferase en qPCR experimenten. Samenvattend kunnen beide VHHs gebruikt worden voor langdurige BMP-7 afgifte. Deze studie suggereert dat Bi3C9 betere karakteristieken heeft en gebruikt zal moeten worden in toekomstige *in vitro* experimenten. Om chondrocyten te targeten in het lichaam, moeten bispecifieke VHHs ontwikkeld worden, die BMP-7 en cel-specifieke eiwitten binden. Deze thesis laat duidelijk zien, dat bifunctionele VHHs gebruikt kunnen worden voor de targeted delivery van BMP-7 *in vitro* en is een veelbelovende strategie als geneesmiddel om het ziekteverloop van artrose te beïnvloeden door de regeneratie van kraakbeen.

Abbreviations

ACAN	Aggrecan
ActR	Activin receptor
ADAMTS	A Disintegrin and Metalloproteinase with Thrombospondin motifs
Bi14F8	BMP7-G7-FSH-14F8
Bi3C9	BMP7-G7-WHR-3C9
BMP-7	Bone Morphogenetic Protein-7
BMPR	BMP Receptor
BSA	Bovine Serum Albumin
CH	Constant Heavy chain
CILP-1	Cartilage Intermediate Layer Protein-1
CL	Constant Light chain
COMP	Cartilage Oligomeric Matrix Protein
DMMB	Dimethylmethylene Blue Assay
ECM	Extracellular Matrix
GAG	glycosaminoglycan
HCAbs	Heavy Chain only Antibodies
ID	Inhibitor of DNA binding
IgG	Immunoglobulin- γ antibodies
ITGB1	Integrin β 1
K_D	Dissociation constant
k_{off}	Dissociation rate
k_{on}	Association rate
MAPK	MAP Kinase
MMPs	Matrix metalloproteinases
NSAIDs	Non-Steroidal Anti-Inflammatory Drugs
OA	Osteoarthritis
PI3K	Phosphatidylinositol-3-kinase
RU	Response Units
SPRi	Surface Plasmon Resonance imaging
TGF- β	Transforming growth factor- β
UCMA	Upper zone of growth plate and Cartilage Matrix Associated protein
VH	Variable heavy chain
VHH	VH of Heavy chain only antibody
VL	Variable light chain

Table of Contents

Abstract

Samenvatting

Abbreviations

1.	Introduction.....	1
1.1	Osteoarthritis.....	1
1.2	Pathogenesis.....	1
1.3	Disease-modifying drugs	3
1.4	Bone morphogenetic protein 7	4
1.5	Antibodies.....	6
1.6	Aim of the research	7
2.	Materials and Methods	8
2.1	Surface Plasmon Resonance.....	8
2.2	Cell culture.....	9
2.3	Immunofluorescence microscopy	9
2.4	Luciferase reporter assay	11
2.5	qPCR.....	13
2.6	Western Blot.....	14
3.	Results	17
3.1	Characterization	17
3.2	Localization	19
3.3	Functionality assays.....	21
3.4	Pathway activation	25
4.	Discussion.....	29
5.	Conclusion	33
6.	Future perspectives.....	34
7.	Bibliography.....	36
8.	Supplementary data	41

1. Introduction

1.1 Osteoarthritis

Osteoarthritis (OA) is one of the most common chronic health conditions and causes major disability worldwide. ¹ Considering the combined effect of increased obesity and aging, the disease is becoming more prevalent with over 303 million people being affected in 2017 globally. ^{2,3} Besides these risk factors, trauma and genetic factors can increase the possibility of getting affected by OA. It is a complex chronic disease, characterized by pain, degeneration in the joints and surrounding tissues, stiffness and swelling resulting in reduced mobility of the patient.

Pharmacologic treatments that are currently available are aimed at pain relief with minimal, if any effect on disease progression. This analgesic medication consists of topical and oral non-steroidal anti-inflammatory drugs (NSAIDs). ⁴ Intra-articular injections of corticosteroids are used as a final non-operative alternative if conventional treatment has proven ineffective, based on current guidelines for knee OA. ⁵ For end-stage OA patients experiencing severe pain, total joint replacement seems to be the only option available at the moment to partially restore joint functionality. ⁶

The damage to the joint is irreversible and therapies for complete prevention or reversing the progression of OA are not available. Unfortunately, diagnosis only occurs after significant symptoms are present in a later stage of the disease. Conventional treatment is largely symptomatic and aimed at providing pain relief and maintaining or improving functioning by applying physiotherapy treatment and lifestyle changes to manage the symptoms. ⁴ In conclusion, there is an urgent need to develop a minimally invasive, disease-modifying treatment for the regeneration of cartilage.

1.2 Pathogenesis

This chapter will provide an introduction to the biology of the joint and the pathogenesis of the disease. Furthermore, disease-modifying OA drugs that can be locally administered are discussed and possible solutions to improve treatment options will be proposed. The aim of this study is addressed in the final part of the introduction.

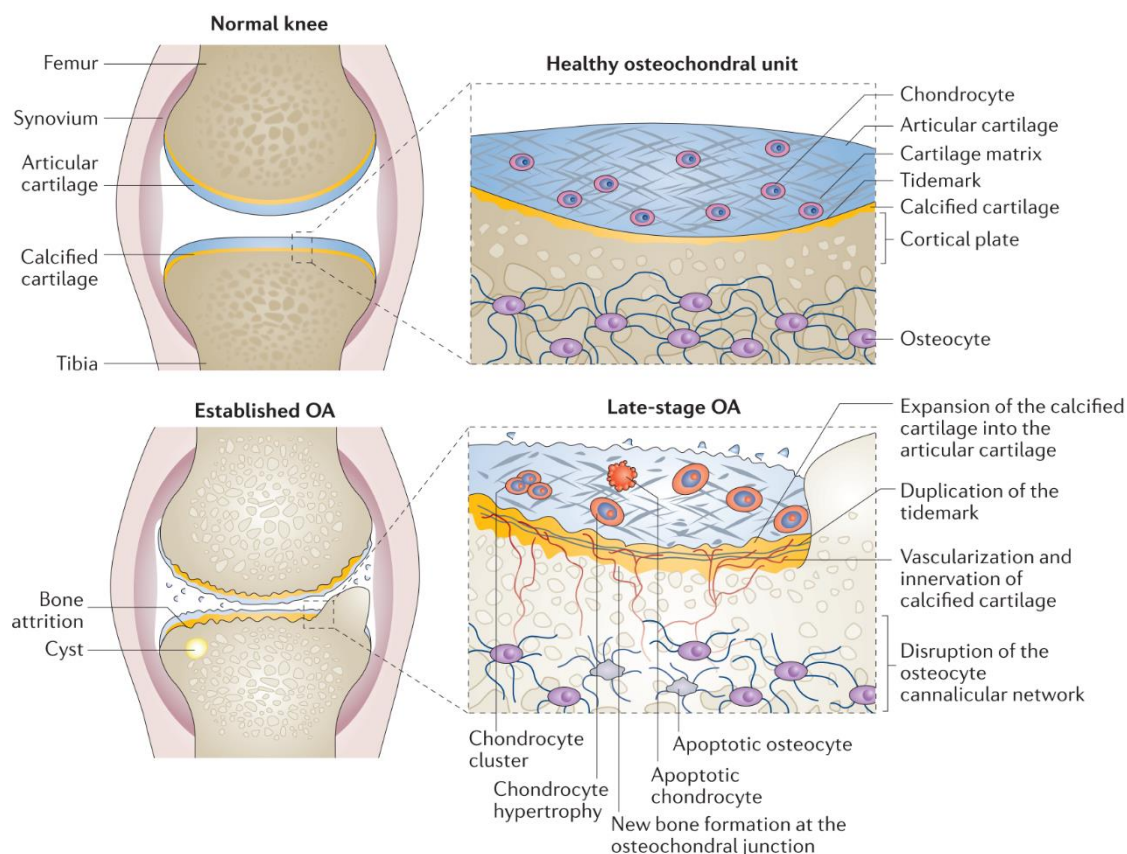


Figure 1: The biology of the joint and pathological changes caused by OA. ⁸

OA is a multifactorial disease that involves the entire joint with alterations of the structure in hyaline articular cartilage, subchondral bone, ligaments, capsule, synovium and periarticular muscles. ⁷ In OA mainly three parts are involved: the articular cartilage, the calcified cartilage and the subchondral bone, also referred to as the osteochondral unit.

The joint ensures frictionless movement between adjacent bones to form a functional unit as depicted in figure 1. ^{6,8} The hard and calcified bones are lined with a thin layer of hyaline cartilage, called articular cartilage. Articular cartilage is an avascular tissue, consisting of chondrocytes at a low cell density and extracellular matrix (ECM) (water, collagen, proteoglycans and a small component of calcium salt). ⁹ Its function is to absorb and distribute the compressive load and shear stress. The chondrocytes are critical for cartilage integrity and maintain a balance by synthesizing the matrix components (collagens and proteoglycans) and the proteolytic enzymes responsible for the breakdown of these components. ¹⁰

The articular cartilage and subchondral bone beneath the cartilage are separated by a thin layer of calcified cartilage. The joint cavity is lined by the synovium. Its function is to produce synovial fluid to provide lubrication and nutrients to the cartilage tissue that helps to maintain joint integrity. ⁶ Ligaments and capsules provide further strength to the joint. ⁸

Although the degeneration and loss of articular cartilage is a prominent feature in the development of OA, the entire osteochondral unit is affected.¹¹ OA pathophysiology is further characterized by subchondral bone remodeling, hypertrophic bone changes and inflammation of the synovial lining.⁶ It is not known what causes the imbalance between degradation and repair of cartilage. Proteolytic enzymes that are involved in the breakdown of for example aggrecan (ACAN) and type II collagen in the ECM components include matrix metalloproteinases (MMPs) and a disintegrin and metalloproteinase with thrombospondin motifs (ADAMTS) enzymes.^{12,13}

As a consequence of this breakdown of ECM, chondrocytes fail to maintain normal homeostasis of the joint between synthesis and degradation of ECM components.¹⁴ The process of joint degradation is accelerated by chronic inflammation, caused by pro-inflammatory cytokines produced by chondrocytes and the synovium.¹⁵

1.3 Disease-modifying drugs

Disease-modifying OA drugs which can be locally administered are being developed to potentially slow down or stop disease progression, or even reverse progression by regeneration of the target tissue.² However, despite many trials, no drugs have been approved yet for this indication according to Hunter et al.²

To preserve cartilage or stimulate its repair, new concepts and techniques to regenerate normal cartilage need to be designed. OA progression can be modified by regulating cartilage anabolism and catabolism, subchondral bone remodeling or synovial inflammation. Growth factors, cytokines, monoclonal antibodies and inhibitors can help to reduce inflammation, promote chondrogenesis, and inhibit osteogenesis and matrix degradation.¹⁶

The regulation of the anabolic effect of chondrocytes plays a crucial role in OA and is therefore an appealing target for novel treatment development.¹⁷ Various studies investigated the use of exogenous growth factors to enhance ECM synthesis as a new therapeutic strategy for cartilage repair and thereby stimulating chondrocyte expansion and re-differentiation. These growth factors include Bone morphogenetic protein-7 (BMP-7), BMP-2, Fibroblast growth factor-18, human serum albumin, insulin-like growth factor-1, Transforming growth factor- β (TGF- β).¹⁸ To date, BMP-7 has proven to be one of the most effective growth factors in enhancing the anabolic activity of adult chondrocytes and will be discussed in more detail in this report.^{19,20}

1.4 Bone morphogenetic protein 7

Bone morphogenetic proteins (BMPs) are a group of signaling molecules that belong to the TGF- β superfamily and play important roles in bone and cartilage formation. The growth factor BMP-7 is interesting as a potential therapeutic target since it, unlike other BMPs and TGF- β , upregulates chondrocyte metabolism and protein synthesis in human chondrocyte cultures, without creating uncontrolled cell proliferation and formation of osteophytes.²¹ Various studies showed an increase in anabolic activity, including the expression of aggrecan and type II collagen.^{22,23} BMP-7 has shown promising results in phase I clinical trials as a treatment for OA.^{24,25} Furthermore, BMP-7 has already been approved for clinical use since 2001 in Europe and Australia for the treatment of non-union bone fractures, which is the failure of a fractured bone to heal.²⁶

BMPs can signal through the canonical, Smad-dependent pathway and via the noncanonical pathway. The signal transduction cascade is initiated by binding to cell surface receptors, forming a hetero-tetrameric complex comprised of two dimers of type I and type II serine/threonine kinase cell surface receptors, shown in figure 2. Both type I and type II receptors have a short extracellular domain to bind BMPs, a single transmembrane domain, and an intracellular domain with serine/threonine kinase activity. BMP binds to three of a total of seven type I receptors (ALK1-7) for the TGF- β family of ligands: type 1A BMP receptor (BMPR-1A) or ALK3, BMPR-1B or ALK6, and type 1A activin receptor (ActR-1A) or ALK2.²⁷ Three of the total of four type II receptors for the TGF- β family are known to interact with BMPs: BMPR-2, ActR-2A, and ActR-2B.²⁸

With regard to the Smad-dependent pathway, BMP-7 has been found to bind to type II (BMPR-II) serine/threonine kinase receptors, recruit and transphosphorylate the type I (BMPR-I) receptor and form a heterotetrameric complex.²⁹ The activated type I receptor phosphorylates intracellular effector proteins, receptor-regulated Smads (Smad1/5/8). This phosphorylated Smad1/5/8 complex associates with co-Smad (Smad4) and is translocated to the nucleus to associate with coactivators to regulate gene expression.²⁸ Extracellular protein antagonists binding to BMP can prevent interaction with receptors (e.g. Noggin). Signaling can also be modulated intracellularly (e.g. FKBP12, microRNAs, phosphatases, and I-Smads) and by co-receptors in the plasma membrane (e.g. Endoglin).²⁸

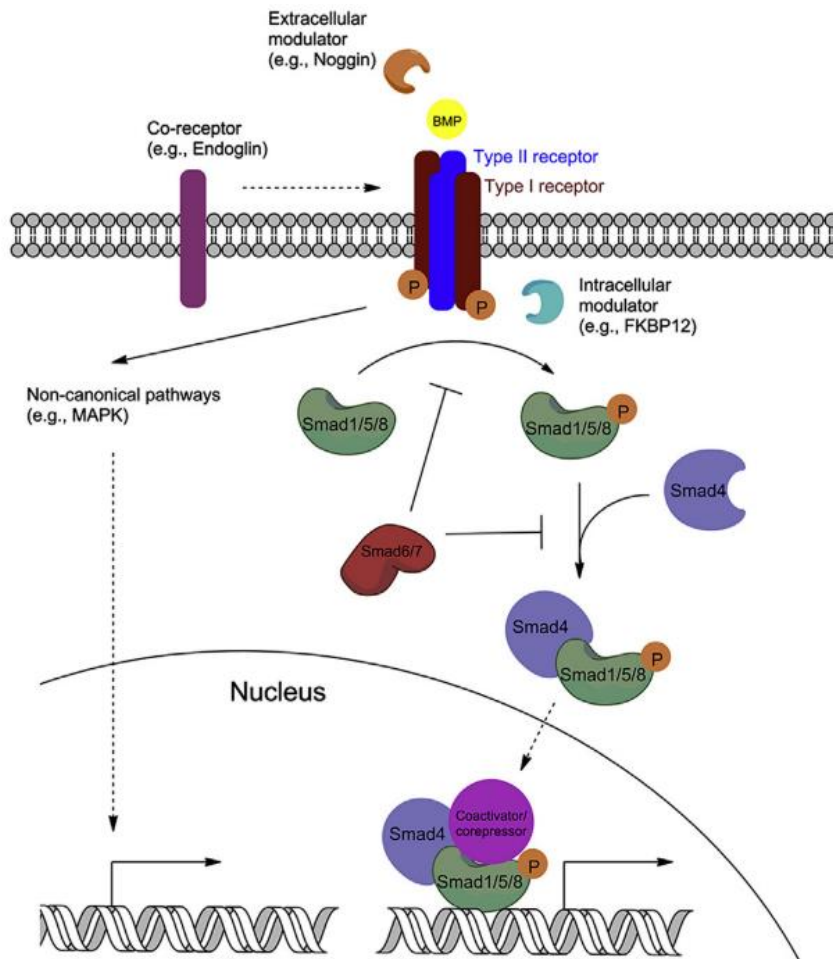


Figure 2: BMP signaling via the canonical (Smad dependent) pathway or the non-canonical pathways. In the Smad-dependent pathway, BMPs bind to type II serine/threonine kinase receptors and forming a heterotetrameric complex. The active type II receptor transphosphorylates the type I receptor and R-Smads (Smad1/5/8) are phosphorylated. This phosphorylated Smad1/5/8 complex associates with co-Smad (Smad4) and is translocated to the nucleus to associate with coactivators to regulate gene expression. Gene expression can also be regulated by various non-canonical pathways, e.g. MAPK. Signaling is modulated extracellularly (e.g. Noggin), intracellularly (e.g. FKBP12, microRNAs, phosphatases, and I-Smads), and by co-receptors in the plasma membrane (e.g. Endoglin).²⁸

In addition to the Smad-dependent pathway, various non-canonical BMP signaling pathways can lead to the regulation of gene expression, including various branches of MAP kinase (MAPK) pathways, Rho-like GTPase signaling pathways, and phosphatidylinositol-3-kinase (PI3K)/AKT pathways.²⁷

The BMP signaling pathway induces the activation of the Smad family members and controls gene expression of the primary target gene: inhibitor of DNA binding (ID), which can be measured after stimulation.³⁰ These ID proteins inhibit the function of basic helix-loop-helix transcription factors, acting as negative regulators of cell differentiation and positive regulators of cell proliferation and cell growth.³¹

As mentioned previously, BMP-7 shows promising results for OA treatment. However, intra-articular injections to deliver this growth factor are not optimal because of the short half-life, low stability and slow tissue penetration.³² Furthermore, BMP-7 is not targeted to the lesion and high doses are needed to reach a biologically relevant concentration to stimulate the chondrocytes.³³ Besides high costs and an unacceptable frequency of weekly injections, these high concentrations can induce adverse side effects and clinical complications.³⁴

Growth factor therapy can be achieved by the administration in a delivery vehicle to enable targeted delivery.¹⁸ Biomaterials can be used for delivery by encapsulating the growth factor or functionalized by covalent coupling.³⁵ Besides the fact that cells are not specifically targeted, the limitation of this method is that growth factors can lose their biological activity during immobilization when functional groups are no longer available for the cells to bind.³⁵

1.5 Antibodies

A more targeted delivery of growth factors to cells can be achieved by using antibodies. The composition and overall structure of antibodies is well conserved among mammals.³⁶ Conventional immunoglobulin- γ antibodies (IgG) consist of two identical pairs of heavy and light polypeptide chains which are linked by interchain disulphide bonds, see figure 3. The light chain consists of one variable domain (VL) at the N terminal end and one constant domain at the C-terminal end (CL). The heavy chain contains one variable domain (VH) and three constant domains (CH 1, 2, and 3).³⁷

Bispecific antibodies containing two different antigen-binding sites have been designed for targeting a tissue to deliver growth factors with high specificity and no modifications needed.³⁸ These conventional antibodies have some limitations, such as large size of approximately 150 kDa for each antigen-binding site, which complicates tissue penetration and results in high cost of production in hosts.^{36,39}

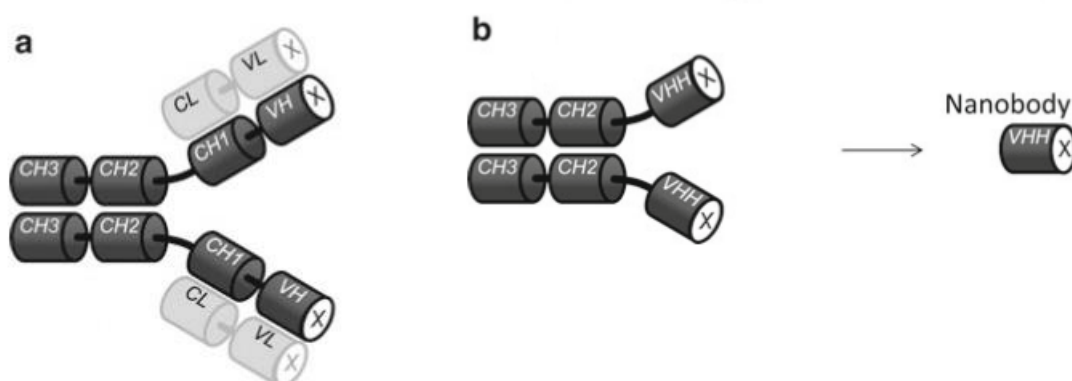


Figure 3: Schematic representation of A) a conventional and B) a camelid heavy chain IgG antibody (HCAbs) and the antigen-binding fragment VHH. The antigen-binding site is denoted by crossed white surfaces.³⁶

A deviation from this large conventional structure can be found in the sera of the family of Camelidae. These antibodies are lacking a light chain and are therefore called heavy chain only antibodies (HCAbs) and are found in addition to the conventional antibodies. The antigen-binding fragment of such heavy chain antibodies can be isolated and is composed of one single domain, the VH of the camelid heavy chain antibody, abbreviated as VHH.³⁶

The advantages of these VHHs are a molecular weight of only 15 kDa that enables efficient penetration of tissues, they are easily cloned and genetically modified and they can be recombinantly produced relatively easy afterwards in bacteria and yeast.³⁹ Furthermore, VHHs remain functional at high temperatures and are expected to be stable at biologically harsh conditions.⁴⁰ VHHs can be fused by an amino acid linker to form a bispecific structure. Bispecific VHHs containing two different antigen-binding sites have been designed for targeting a tissue to deliver growth factors with high specificity and no modifications needed.³⁸ To enable the controlled delivery of BMP-7 from a VHH as a possible therapy for OA, we aim to create a bispecific VHH. In this bispecific VHH, one VHH clone functions to target a tissue-specific protein, and the other VHH clone targets BMP-7 for a potential therapeutic strategy.

1.6 Aim of the research

At this moment, no successful disease-modifying treatment for the regeneration of cartilage in OA is available. The research question of this proof of principle study is to determine whether it is possible to influence the BMP-7 pathway with a bispecific VHH that targets both the cell adhesion receptor integrin $\beta 1$ (ITGB1) and BMP-7, by locally enhancing the BMP-7 concentration. Integrins are heterodimeric cell surface molecules that link the internal signaling components of the cytoskeleton to the extracellular microenvironment.⁴¹ ITGB1 is a major cell surface receptor responsible for cell adhesion, which has been reported to be expressed on the surface of chondrocytes.⁴² Since the experiments in this proof of principle study were conducted on cultured cells *in vitro*, ITGB1 was chosen as a target to show the effect of BMP-7 stimulation in 2D cell culture.

To answer the research question, several experiments were performed. To determine the affinity of the bispecific VHHs for their targets, surface plasmon resonance imaging (SPRi) measurements were done. To localize and confirm binding and dual binding, immunofluorescence assays were performed. The effect of the VHHs on the bioavailability was determined with a luciferase assay and described as blocking, neutralizing, or no effect. To assess pathway activation after BMP-7 stimulation in the presence or absence of VHHs, the effect on gene expression and protein phosphorylation was determined with qPCR and western blot assays respectively.

2. Materials and Methods

This project was part of an ongoing collaboration between the Developmental BioEngineering group at the University of Twente, QVQ and Orthros Medical. To target ITGB1, two different VHHs WHR-3C9 (mono3C9) and FSH-14F8 (mono14F8) were used. These two clones targeting ITGB1 were fused with BMP7-G7 to form a bispecific VHH (Bi14F8 and Bi3C9), by genetic fusion with a flexible GS linker.

2.1 Surface Plasmon Resonance

The binding affinities for ITGB1 and BMP-7 of the bispecific VHHs were measured using SPRi. The protocol is based on the article by Hendriks et al.⁴³

The bispecific VHHs BMP7-G7-WHR-3C9 and BMP7-G7-FSH-14F8, BMP7-G7, and bovine serum albumin (BSA) (Sigma-Aldrich) were immobilized on G-type Easy2Spot sensors (Ssens BV) at 256, 128, and 64 nM, using the Wasatch microfluidics continuous flow spotter for 30 minutes (Wasatch Microfluidics). The immobilization reaction was performed in 50 mM acetic acid buffer (Sigma-Aldrich) with a pH of 4.6 to provide the highest retained activity of the coupled antibodies. The sensor was deactivated with 1% BSA in 50 mM acetate buffer at pH 4.6 for 7 min and subsequently with 0.2 M ethanolamine (Sigma-Aldrich) at pH 8.5 for 7 min, to reduce nonspecific interactions.

The IBIS MX96 (IBIS technologies) was used for the SPRi measurements. To determine the shift in the SPR angle, it applies an angle-scanning method with automatic fitting. Suit software (IBIS Technologies) was used to program the type of interaction, interaction times, samples, and regions of interest (ROIs) for the antibodies. The IBISMX96 provides automatic liquid handling and SPR angle measurements. Before the experiments were performed, angle offset was applied to ensure a wide dynamic detection range. 48 sensor spots were used in every experiment. Back-and-forth flow was set to 10 μ L/min in a flow cell containing 12 μ L of sample, which enables minimal sample use.

The analytes ITGB1 (Sinobiological, 10587-H08H1) and BMP-7 (RnD systems, 354-BP-010) (at a concentration of 2, 4, 8, 16, 32, 64, 128, and 256 nM) were dissolved in system buffer, containing phosphate-buffered saline (PBS) (Sigma-Aldrich) with 0.075% Tween 80 (Sigma-Aldrich, P1745). The affinity between the VHHs on the sensorchip and the analytes was determined by applying the kinetic titration method to avoid possible reduction in binding capacity under regeneration conditions.⁴⁴ First two blanks were injected, followed by the lowest analyte concentration of 2 nM and successive injections with doubled concentrations up to 256 nM. The association time of each interaction was 15 min followed by a 20 min dissociation. After every injection, system buffer was used for washing. After the

measurements, data was collected and processed with Sprint software and exported to Matlab R2016a for analysis using custom scripts designed by J. Hendriks.⁴³ The blanks were subtracted and the signal was zeroed to the first interaction. Deviations of the fitting curve from the actual data were determined using residual plots. The signal of four independent spots was averaged and 1:1 fitting showed not appropriate due to a biphasic pattern.⁴⁵ Therefore, a more complex model was used where both fast and slow interactions were taken into account.

2.2 Cell culture

In this study, two different types of cell lines were used. The human chondrocyte immortalized cell line C-20/A4 was provided by Dr. Mary Goldring, Hospital for Special Surgery, New York.⁴⁶ Cells were cultured at 37°C and 5% CO₂ in the incubator, in Dulbecco's modified Eagle's medium (DMEM) (Gibco, 41965-039) containing 10% fetal bovine serum (FBS) and 1% penicillin/streptomycin (pen/strep) (Sigma Aldrich). C-20/A4 cells were seeded at 3000 cells/cm². Cells were used for immunofluorescence, qPCR, and western blot.

The mouse muscle myoblast cell line C2C12 was transfected previously with a BRE-Luc construct (BMP responsive gene fused to a luciferase reporter gene) (ATCC CRL-1772). Stimulation with BMP induces luciferase expression. The cells were used for immunofluorescence assays and the luciferase assay. Cells were cultured in DMEM supplemented with 20% FBS and 1% pen/strep.

Cells were passaged twice a week, reaching maximal confluency of 70-80%. When passaging or plating the cells, the cells were washed with PBS (Lonza, BE17-516F) and incubated with trypsin-EDTA 0.25% (Gibco) for 5 minutes in the incubator.

2.3 Immunofluorescence microscopy

Immunofluorescent assays were conducted to show the binding of the VHHs to ITGB1 expressed on the cell membranes of C2C12 BRE-Luc cells. First, 15 mm diameter coverslips were disinfected using 70% ethanol and placed in every well of a 24 wells plate (Greiner Bio-One, 662160). After rinsing twice with PBS, the coverslips were coated with 5µg/cm² fibronectin for 1 hour at 37°C. The coverslips were washed twice and cells were cultured for 2 days in DMEM 20% FBS and 1% pen/strep at a seeding density of 7500 cells/cm².

After two days of culturing the cells on the coverslips, the immunofluorescent assays were performed. The cells were washed twice in cold PBS before and after fixation with 4% paraformaldehyde (Sigma-Aldrich, 30525-89-4, P6148) for 5 minutes. In between incubation steps, the cells were washed with PBS two times quickly and three times for five minutes. The

coverslips were placed in a petri dish containing wet tissue and Parafilm M to prevent dehydration. The cells were permeabilized with 1% BSA and 0.1% Triton in PBS for 15 min at room temperature.

Subsequently, the cells were incubated with 100 nM VHH in 1% BSA and 0.1% Triton in PBS for 60 minutes at 37°C. WHR-3C9, FSH-14F8, and both bispecific VHHs were used. Nonspecific DKK1 and no VHH were included as negative control and human integrin beta 1/CD29 antibody (RnD, MAB17781) was used as positive control.

To detect the binding of the VHHs towards ITGB1, the coverslips with VHHs and the negative controls were incubated first with 2 µg/ml rabbit-anti-VHH (purified) (QVQ, 20180912UTK) in PBS containing 1 mg/ml BSA + 0.1% Triton for 60 min at 37°C. The secondary antibody, 2 µg/ml goat-anti-rabbit conjugated with Alexa Fluor 488 (Invitrogen, A-11008) was incubated together with Phalloidin Alexa Fluor 647 (Invitrogen, A22287) in PBS with 1 mg/ml BSA and 0.05% Triton for 30 minutes at 37°C. To detect the binding of the positive control, 1 µg/ml donkey-anti-mouse conjugated with Alexa Fluor 488 (Abcam) was incubated together with 0.165 µM Phalloidin Alexa Fluor 647 in PBS with 1 mg/ml BSA and 0.1% Triton for 60 minutes at 37°C.

All coverslips were incubated with 5 ng/ml DAPI (Thermo Scientific, 62248) staining in PBS with 1 mg/ml BSA and 0.05% Triton for 5 minutes at room temperature to stain the cell nucleus. The coverslips were mounted with Fluorsave Reagent (Calbiochem) on microscope slides at room temperature for at least 1 hour. The confocal microscope (Nikon A1) with lasers 405, 488, and 647 was used to image the samples.

To show that binding takes place in human chondrocytes as well, the immunofluorescence protocol described above was conducted using C-20/A4 cells. Cells were seeded at 5000 cells/cm² and cultured for one day. The cells were incubated with Bi14F8 only to check if binding occurred. Nonspecific DKK1 and no VHH were included as negative control and human integrin beta 1/CD29 antibody was used as positive control. Instead of DAPI, Hoechst 33342 (RnD, 5117) was used at a concentration of 1 µg/ml.

Bifunctional immunofluorescence

Immunofluorescence was used as well to determine if the VHHs can bind ITGB1 and BMP-7 simultaneously. The C2C12 BRE-Luc cells were cultured, fixed and permeabilized as described above. The bispecific VHH (100 nM) were first pre-incubated with equimolar BMP-7 for 1 hour in PBS with 1 mg/ml BSA and 0.1% Triton. Besides the pre-incubated VHHs, coverslips were incubated with 100 nM free BMP-7, the bispecific VHH or no VHH for 60 minutes at 37°C. After blocking with BSA for 15 minutes, 8 µg/ml mouse anti-human BMP-7 antibody (RnD Systems, MAB3541) in PBS with 1 mg/ml BSA and 0.1% Triton was incubated for 60 minutes at 37°C

followed by 30 minutes incubation with 2 µg/ml donkey-anti-mouse conjugated with Alexa Fluor 488 together with 0.165 µM Phalloidin Alexa Fluor 647, in PBS with 1 mg/ml BSA and 0.05% Triton at 37°C. The cells were incubated with DAPI staining, mounted with Fluorsave reagent, and imaged with the confocal microscope as described above.

Cell-matrix interaction

To determine if the binding of the VHHs towards ITGB1 affects the morphology and binding of C2C12 BRE-Luc cells, fluorescent tracking was used. Cells were harvested using trypsin-EDTA 0.25% as described before and resuspended in 5 µM pre-warmed CellTracker Green CMFDA (Thermo Scientific, C2925) diluted in serum-free DMEM. The CellTracker solution was incubated for 15 minutes at 37°C, after which 22 µM Hoechst 33342 (Thermo Scientific, H3570) was added for 15 minutes. The cells in suspension were centrifuged to remove the CellTracker solution and seeded at a density of 7500 cells/cm² in DMEM 20% FBS and 1% pen/strep, together with WHR-3C9, FSH-14F8, the bispecific VHHs, human integrin beta 1/CD29 antibody or no VHH. After 1 day, the confocal microscope was used to determine the attachment of the cells. ImageJ was used to measure the circularity of the cells.

2.4 Luciferase reporter assay

To determine the effect of the bispecific VHH on the bioactivity of BMP-7, a luciferase reporter assay was performed, using the C2C12 BRE-Luc cells. The C2C12 cell line was stably transfected previously with the BRE-Luc construct which contains the BMP-responsive elements of the mouse ID1 gene, cloned into the pGL3 luciferase vector.⁴⁷ ID1 is a direct target gene for BMP. BMP strongly activates the ID1 promoter in a SMAD-dependent manner, whereas TGB-β does not activate this promoter.⁴⁷

Optimization of the BMP-7 concentration

An optimization assay was performed to choose the correct human BMP-7 concentration to use in the luciferase reporter assay for a significant increase compared with the negative control. The cells were cultured overnight in a 24 wells plate at a density of 10000 cells/cm² in DMEM with 20% FBS and 1% Pen/Strep. To minimize the influence of the culture medium and to synchronize all cells to the same cell cycle phase, starvation of the cells was performed for 10 hours in DMEM 1% FBS and 1% Pen/Strep. Stimulation of the cells was done for 14 hours with human BMP-7 in starvation medium at a concentration of 0.1, 1, 10 and 100 ng/ml. After stimulation, the cells are lysed with 1X Reporter Lysis Buffer (RLB) from the Promega luciferase assay kit (Promega, E1500). After one freeze/thaw cycle (15 minutes at -80°C and 30 minutes at room temperature) the samples were vortexed for 10 seconds and centrifuged in 1.5 ml

Eppendorf tubes for 2 minutes at 4°C at 12000 rcf to remove cell debris and the supernatant was transferred to new Eppendorf tubes for the measurements.

To measure the luminescence of the luciferase assay, the Victor³ multilabel plate reader (PerkinElmer) was used with the Hugo/Stein 10 sec. luciferase protocol, which has been designed before with the appropriate delay and measurement times. The luciferase content per sample was determined for each triplicate by adding 20 µl of the sample (with a delay of 12 seconds in between samples) to 100 µl of the luciferase assay reagent (Promega, E1500) in white 96 well plates (Corning, 3917).

The DNA content per sample was determined to correct the luminescent measurement for the amount of cells per sample. After warming all assay components to room temperature, 200 µl of the Quantifluor dsDNA dye (Promega, E2670), diluted 400 times in 1X TE buffer (Promega, E2670) was added to each well of the black 96 wells plate (Corning, 3603), intended for an unknown, blank or standard sample. A standard curve was created by adding 10 µl of the Lambda DNA (Promega, E2670) concentrations 20, 5, 1.25, 0.31, 0.078, 0.02, and 0.005 ng/µl in 1X TE buffer to the Quantifluor dsDNA dye. For the unknown samples, 20 µl was added to the wells plate. After incubation of the plate at room temperature for 5 minutes on a plate shaker, the fluorescence was measured with the Victor³ multilabel plate reader at an excitation wavelength of 504 nm and an emission wavelength of 531 nm. The fluorescence of the 1X TE buffer blank sample was subtracted from all standard and unknown samples. The DNA content of each unknown sample was calculated, using the QuantiFluor Dye Systems Data Analysis Workbook.⁴⁸ Using these DNA concentrations, the average luminescence corrected for the DNA content was determined for every condition.

Effect of the VHHs on the bioactivity of BMP-7

Using the optimization assay, 10 ng/ml human BMP-7 was chosen as a suitable concentration to determine the effect of the VHHs on the bioactivity of BMP-7. The same protocol as described above was used. The stimulation was performed with BMP-7 (10 ng/ml, 0.637 nM), BMP-7 with equimolar bispecific VHH (0.637 nM), BMP-7 (0.637 nM) with VHH in excess (6.37 nM or 63.7 nM), only bispecific VHH (0.637 nM) and the negative control with unstimulated cells. The conditions BMP-7 with equimolar VHH and 10 and 100 times excess of the VHHs were tested with pre-incubation for 1 hour at RT and without pre-incubation.

Long term release luciferase assay

Since the experiment described above only determines the effect of the VHH on the bioactivity at one time point and BMP-7 and VHH were added simultaneously, another experiment was designed to assess the long term release of BMP-7 from the bispecific VHH. To this end, the stimulation was changed by first incubating the bispecific VHH in the corresponding conditions

for 30 minutes at 37°C. After washing with PBS, the BMP-7 was incubated for 30 minutes at 37°C. Fresh starvation medium was added after washing and the stimulation was performed for 14, 24, 48 and 72 hours to determine if the release over time is different from the stimulation with BMP-7 only. Considering the washing step, 30 ng/ml BMP-7 was chosen instead of 10. The stimulation was performed with BMP-7 (30 ng/ml, 1.911 nM), BMP-7 with equimolar bispecific VHH (1.911 nM), BMP-7 (1.911 nM) with VHH in excess (19.11 nM or 191.1 nM), only bispecific VHH (1.911 nM) and the negative control with unstimulated cells.

The negative control was set to one to determine the fold change of the stimulated conditions relative to the control. The results of the last two experiments were tested for significance with GraphPad Prism 8 using one-way ANOVA and Tukey's multiple comparisons test.

2.5 qPCR

To determine the genes which are overexpressed after stimulation with human BMP-7, qPCR was performed using the human chondrocyte cell line C-20/A4. The cells were cultured in 12 wells plates (Greiner Bio-One, 665180) at a density of 5000 cells/cm² for three days. After starvation for 10 hours, the cells were stimulated for 6 and 24 hours with BMP-7 (40 ng/ml, 2.55 nM), only the bispecific VHH (2.55 nM), BMP-7 with equimolar bispecific VHH (2.55 nM), and the negative control starvation medium (DMEM with 1% pen/strep).

The RNA was isolated using the NucleoSpin RNA kit (Machery Nagel, 740955.250). The reducing agent β -mercaptoethanol (Gibco, 31350010) was added as supplement for Lysis Buffer RA1. Cell-culture medium was completely aspirated and Lysis Buffer RA1 was added to the wells plate. Then, RNA was obtained by lysis and isolation according to the manufacturer's instructions described in the RNA isolation user manual.⁴⁹ The RNA was eluted in 40 μ l RNase-free water in the final step.

Subsequently, the RNA concentration and the purity were measured with the Nanodrop ND-1000 UV-Vis Spectrophotometer (Thermo Scientific). First, 1.5 μ l RNase-free water was measured as blank sample. The eluates were measured in the same manner, using a Kimwipe tissue to blot dry the pedestals. The RNA was diluted with water to reach an equal concentration in every condition by using 1 μ g of each sample in 15 μ l. Nuclease-free water was serving as a No Template Control. The iScriptTM cDNA Synthesis Kit (Bio-Rad, 1708891) was used to synthesize cDNA. The iScript master mix was prepared, containing 1 μ l iScript Reverse Transcriptase and 4 μ l 5x iScript Reaction Mix per sample, which was added to the tubes with the RNA samples and to the No Template Control. In the No Amplification Control, one sample or a mixture was used, where the 1 μ l iScriptReverseTranscriptase enzyme was replaced by Nuclease-free water and 4 μ l of 5x iScript Reaction Mix was added.

The samples were loaded in a qPCR 96 wells plate (Bio-Rad, HSS9641), the plate was sealed with AluminumSeal (VWR, 732-7505) and centrifuged for 1 min at 4000 rcf. The BioRad CFX96 was used for cDNA synthesis using the following protocol: 5 minutes at 25°C, 30 minutes at 42°C, 5 minutes at 85°C, and hold at 4°C. The samples were diluted to 0.625 ng/ml with RNase free water. For the qPCR analysis, the housekeeping gene B2M and the genes of interest RUNX2, TCF1, LEF1, SOX9, and ID1 were used. The qPCR master mix was added to every well of the qPCR 96 wells plate, consisting of 1 µl forward primer, 1 µl reverse primer, and 10 µl SensiMix™ SYBR® & Fluorescein (2X). All samples were measured in duplicate. The diluted cDNA (8 µl) was added and the plate was sealed to prevent evaporation. After spinning the plate down using the Eppendorf centrifuge for 1 minute at 4000 rcf, the plate was loaded into the BioRad CFX96, running the following program: 1 hot start of 95°C for 10 minutes, followed by 40 cycles of 15 seconds melting at 95 °C, 15 seconds annealing at 60 °C (depending on the primer), 15 seconds extension at 72 °C and followed by a melting curve from 65°C to 95°C (5s/°C).

For analysis of the qPCR results, all genes of interest are normalized to the housekeeping gene B2M. Primers for the genes are specified in the supplementary data, table 1. After normalization, the fold induction compared to the negative control was calculated.

2.6 Western Blot

To decide on a protein level the effect of BMP-7 stimulation, western blot analysis was used. Phosphorylated and normal Smad were detected to determine the effect of BMP-7 stimulation. Furthermore, phosphorylated and normal FAK were analyzed to determine the possible effect of the binding of VHHs to ITGB1.

The cells were cultured in 6 wells plates and stimulated for 15 minutes, 30 minutes, 1 hour and 2 hours with the stimulation conditions described in the qPCR chapter. After washing the cells with PBS, the cells were lysed on ice for 5 minutes, using 300 µL of a mixture of cold radioimmunoprecipitation assay (RIPA) lysis buffer (Thermo Scientific Pierce, 89900) and 1X HALT Protease and phosphatase inhibitor (Thermo Scientific, 78444). The lysate was transferred to a microcentrifuge tube and centrifuged at 4°C for 15 minutes at 14000 rcf. The supernatant was divided over 3 Eppendorf tubes and stored at -80°C.

To determine the protein content of the samples, the BCA Protein Assay Kit (Pierce) was performed according to the manufacturers' user guide.⁵⁰ A Matlab script provided by Marieke Meteling was used to calculate the protein concentration of the samples, using the diluted BSA standard range. A mixture of 1X Laemmli buffer and 5mM beta-mercaptoethanol was added to 10 µg of protein from each sample (1:3 ratio sample:buffer). After puncturing the tube lids with a syringe needle and heating the samples for 5 minutes at 95°C, the samples were loaded in the SDS-PAGE precast gels (Bio-rad Mini-PROTEAN TGX Gels, 4561084) in the

Mini Protean Tetra Cell tank (Bio-Rad 552BR), using 1x SDS running buffer. The protein marker Precision Plus Protein WesternC Blotting Standards (BIO-RAD, 1610376) was added to the outer slots (5 µL). The gels were runned at 15 mA constant current per gel until all samples were in the running gel, followed by running at 30 mA per gel until the dye front is at the bottom of the gel.

The gel was retrieved from the electrophoresis module and placed between the Trans-Blot Turbo Transfer Pack (Bio-Rad, 1704156), according to the manufacturers' instructions. The Turbo protocol was selected, using the Trans-Blot Turbo Transfer System (Bio-Rad). The PVDF membranes were marked with a pencil to distinguish the protein side of the membrane and placed in 50 ml tubes containing 5ml blocking buffer (PBS with 0.1% Tween (Sigma, slcf5974) with 5% BSA) and incubated for 30 minutes at room temperature. The solution was replaced with fresh blocking buffer and 5 µl of the first antibody was added and incubated overnight at 4°C under constant mixing.

After washing with PBS Tween 0.1% 6 times for 10 minutes, the membranes were placed in tubes for 1 hour at room temperature with the second antibody solution, consisting of 2,5 µL secondary antibody conjugated HRP (polyclonal goat anti-rabbit(DAKO, p0448) and polyclonal goat anti-mouse(DAKO, p0447)) and 0.5 µL StrepTactin-HRP-conjugate in 5 mL of washing solution, followed by 6 times 5 minutes washing. The antibody complex was detected using an HRP substrate SuperSignal West Femto Maximum Sensitivity (Thermo scientific, 34096), mixing equal parts of the Stable Peroxide Solution and the Luminol/Enhancer Solution.

The FluorChem M imager with chemiluminescence was used for the detection of the bands on the membranes. The membrane was washed three times for 5 minutes to remove the substrate and stripped to remove the bound first and second antibody, using Restore PLUS Western Blot Stripping Buffer (Thermo Scientific, 46430) for 30 minutes at 37°C and washing extensively afterwards. For the next first antibody, the protocol was continued with the blocking as described before.

For the detection of the phosphorylated SMAD protein and FAK, TBS-Tween 0.1% was used instead of PBS Tween in the washing and blocking buffer described above. TBS consists of 0.2M Tris-base, 1.5M NaCl, and 0.1%Tween 20 in MilliQ, with a pH of 6.8 adjusted by adding 12M HCl. The first antibodies used were Rabbit Monoclonal antibody Phospho-Smad1(Ser463/465)/Smad5 (Ser463/465)/ Smad9 (Ser465/467) (Bioké, 13820S) and Rabbit polyclonal antibody to pFAK (Santa Cruz, sc-101680).

Rabbit polyclonal antibody to Smad1/5/8 (Santa Cruz, sc-6031-R), Mouse monoclonal antibody to FAK (Santa Cruz, sc-271126), and Mouse monoclonal antibody to beta Actin (Abcam, ab82226) were detected following the protocol described above with PBS Tween.

The intensity of the bands was analyzed using ImageJ and standardized to the intensity of Beta-actin.

3. Results

In this chapter, the obtained results of the experiments as described in chapter 2 are shown. The experiments were designed to determine if cells can be self-stimulated by using bispecific VHHs and BMP-7. In this proof of principle study, ITGB1 was targeted with FSH-14F8 or WHR-3C9 to be able to determine the effect of BMP7-G7 on BMP-7 accumulation *in vitro* in 2D cultures.

To determine the affinity of the bispecific VHH for their targets, SPRi measurements were done. To localize the binding of the VHHs and confirm binding and dual binding, immunofluorescence, and confocal microscopy were performed. The effect of the VHHs on the bioavailability of BMP-7 was assessed with the luciferase reporter assay and pathway activity was determined with qPCR and western blot to see which genes are overexpressed after BMP-7 activation and which proteins are phosphorylated.

3.1 Characterization

SPRi analysis was used to determine the binding affinity between the VHHs and ITGB1 or BMP-7. The VHHs were immobilized on the surface of the sensor. A concentration range of the analyte was used to measure the dissociation rate (k_{off}) and association rate (k_{on}). Subsequently, the dissociation constant (K_D) value was determined.

Characterization by SPRi showed that Bi14F8 and Bi3C9 both have a high affinity for ITGB1 and BMP-7. The BMP7-G7 targeting BMP-7 showed no binding to the ITGB1 analyte as expected and a high affinity for BMP-7. Figure 4A and 4B show the interaction of both bispecific VHHs as well as BMP7-G7, using concentrations of 128 nM and analyte concentrations of 256 nM to show the binding pattern.

The fitting of the signal showed the best result using a model where both fast and slow interactions were taken into account. This binding pattern is distinctive for a biphasic reaction.⁴⁵ Analysis results in 2 values for the k_{off} , k_{on} , and K_D for every spot concentration, using a concentration range of the analyte. The weighted K_D is used to describe the binding affinity of the VHH towards the analyte. Both bispecific VHHs show a high affinity in the range between 100 nanomolar and 1 picomolar for BMP-7 and ITGB1 values are described in figure 4C. All k_{off} , k_{on} , and K_D values are shown in Table 2 and 3 of the supplementary data.

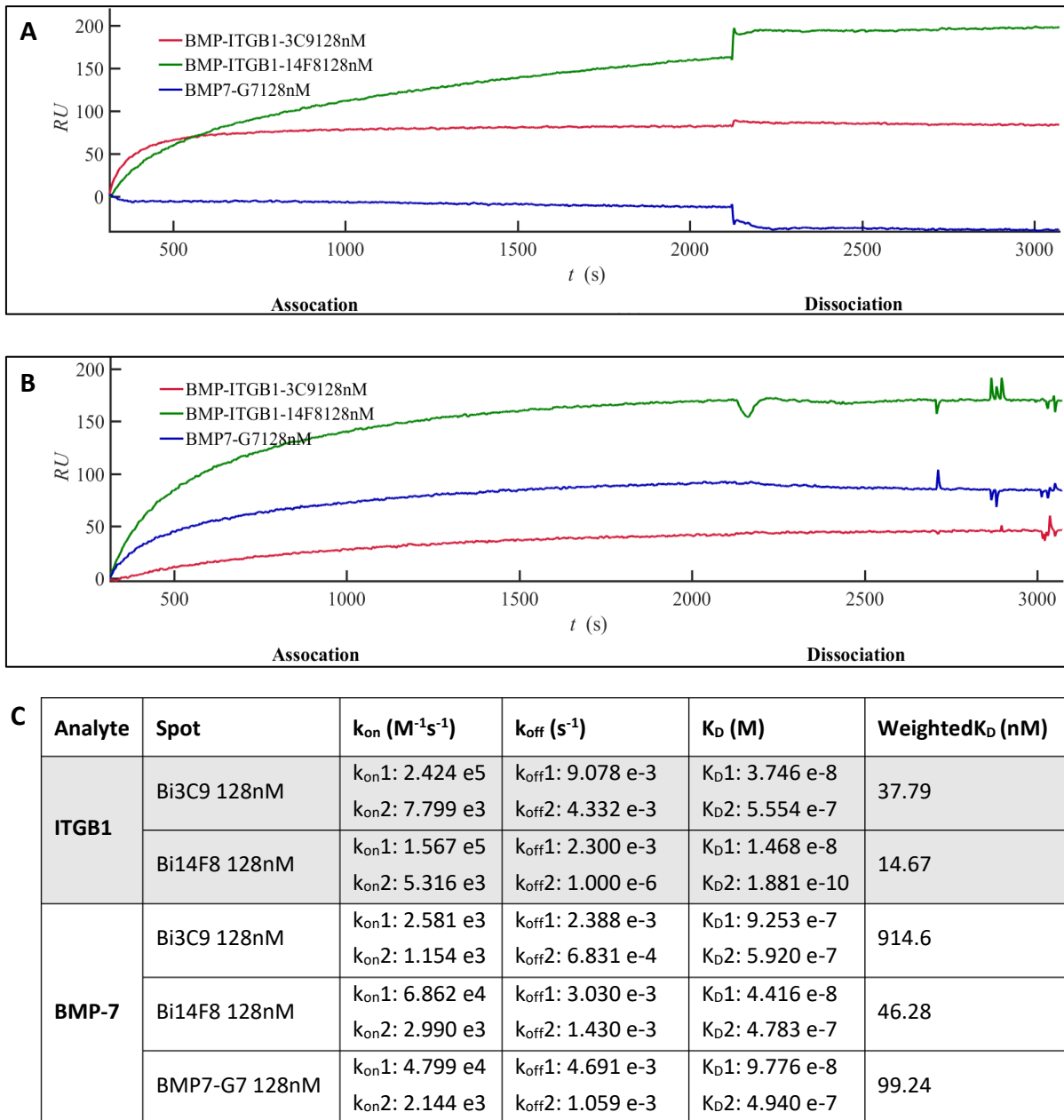


Figure 4: SPRi results of the interaction of both bispecific VHHs as well as BMP7-G7, using concentrations of 128 nM. Analyte concentrations of 256nM were shown to visualize the binding pattern of A) ITGB1 and B) BMP-7. C) The k_{on} , k_{off} , K_D , and weighted K_D of the same spots are shown, determined with the analyte dilution range between 2 nM and 256 nM.

Important to note is that the complex is very stable in the dissociation phase, resulting in a low k_{off} . Since the affinity towards ITGB1 is high, the VHHs are suitable for targeted delivery in this proof of principle study. In addition, the binding affinity of anti-BMP-7 of the bispecific VHH is rather high and further experiments need to be conducted to see if this VHH is able to sequester BMP-7 without neutralizing the growth factor.

3.2 Localization

To investigate the subcellular localization, FSH-14F8, WHR-3C9, Bi3C9 and Bi14F8 were incubated and immunofluorescence assays were performed. The immunofluorescence assay of VHHs bound to ITGB1 on C2C12 BRE-Luc cells was successful and shown in figure 5.

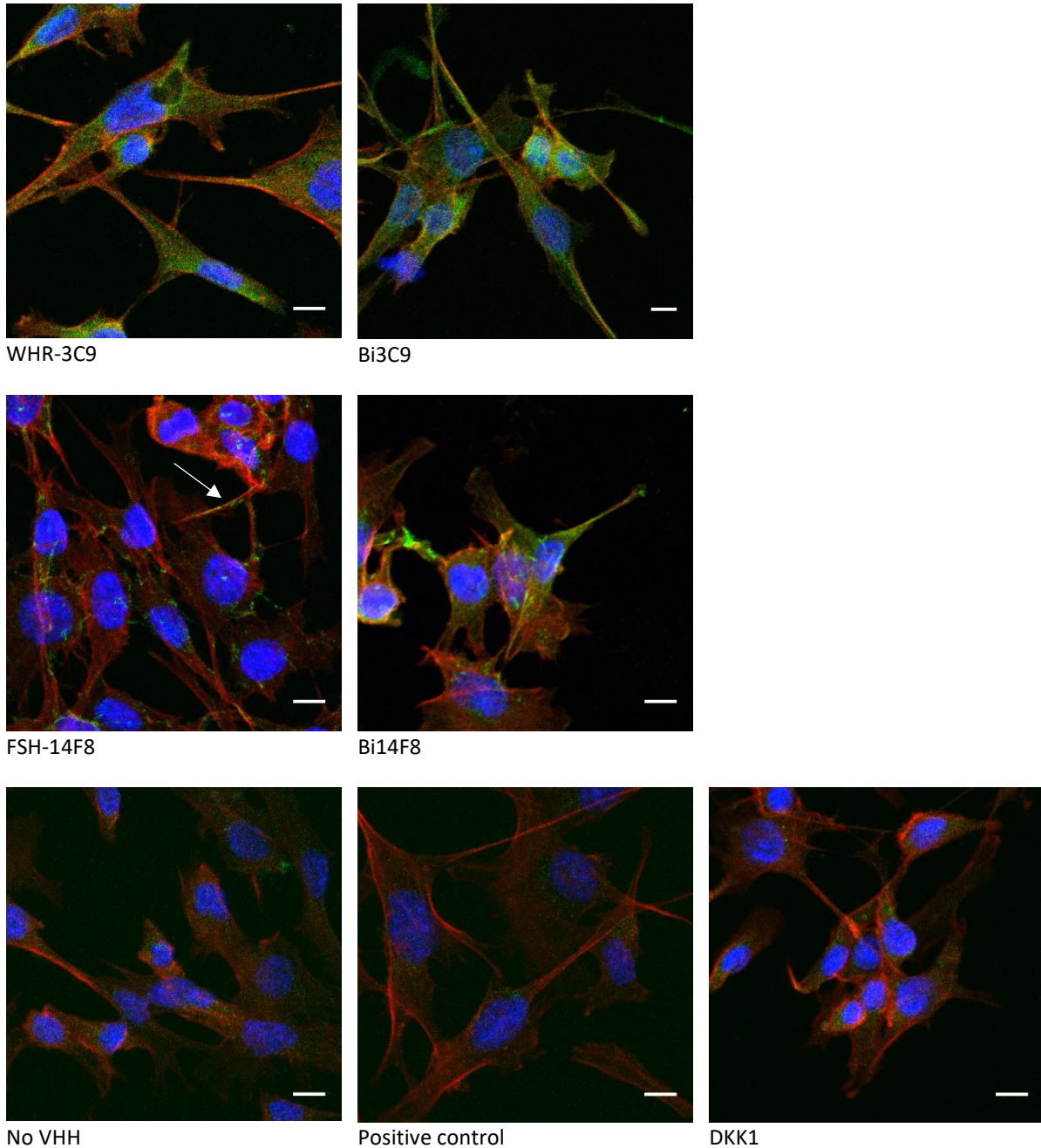


Figure 5: Membrane staining to localize VHH binding on fixed C2C12 BRE-Luc cells. Adherent cells were fixed with formaldehyde, and incubated with VHH as primary antibody, as indicated in the figure. VHHs were detected by a secondary antibody coupled to Alexa Fluor 488 (green). The positive control is mouse monoclonal antibody against human ITGB1. The α -specific VHH DKK1 is a central regulator of osteoblast activity and was used as negative control. The arrow indicates localization at focal adhesions. Nuclei were counterstained with DAPI(blue) and the actin filaments with Phalloidin (red). Scale bar is 10 μ m, objective 20x.

It is clear that the localization of the binding of the VHHs is different. The binding of FSH-14F8 and Bi14F8 results in a spotted green signal and occurs near the focal adhesions of the cell or the cell junctions, indicating transmembrane or membrane-associated proteins as antigens. The binding of WHR-3C9 and Bi3C9 did not result in this specific pattern and shows diffuse staining around the nucleus. No green VHH signal was observed in the negative controls DKK1 and no VHH, as expected. A mouse monoclonal antibody against human ITGB1 was used. Despite the fact that there is a high resemblance between mice and human ITGB1 of 92.5%, the staining in the positive control was absent. ⁵¹

Although the quality of the staining of the samples was poor in comparison with the previous experiment and only a few cells were stretched, figure 6 only indicates that the staining procedure was successful on C-20/A4 cells and Bi14F8 was able to bind ITGB1. Since the binding location was already visualized in C2C12 BRE-Luc cells, only one VHH was used to confirm binding in this cell type. The negative controls show no binding of the VHH as expected. Again, the positive control in this human chondrocyte cell line is negative. The secondary antibody conjugated to Alexa 488 that was used, showed fluorescence as expected (data not shown). To be certain the antibody is not functional in human cells, the experiment has to be repeated considering the poor sample quality. In conclusion, the binding location was successfully visualized in C2C12 BRE-Luc cells.

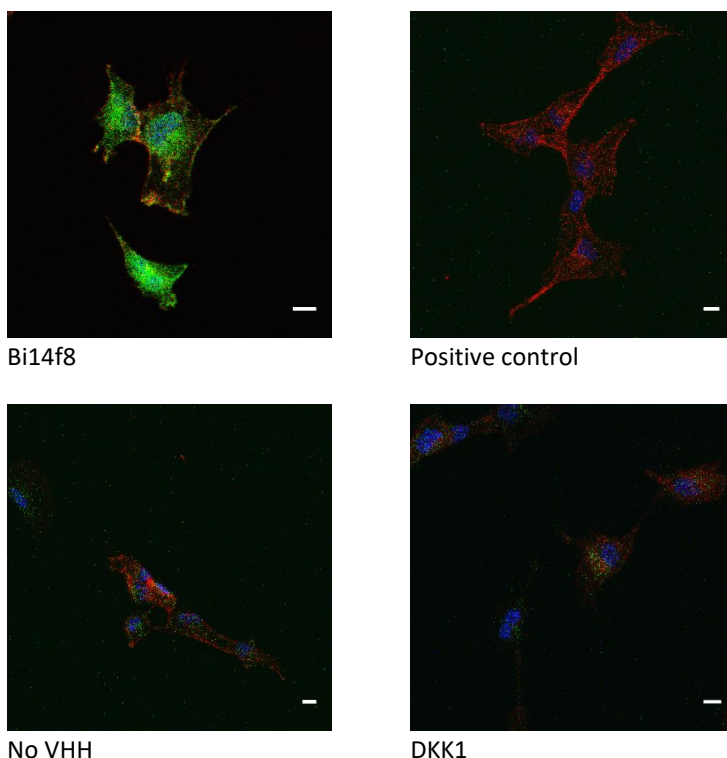


Figure 6: Membrane staining to confirm VHH binding on fixed C-20/A4 cells. Cells were adhered to cover slides, fixed with formaldehyde, and incubated with VHH as indicated in the figure, as primary antibodies. VHH were detected by a secondary antibody coupled to Alexa Fluor 488 (green). The positive control is mouse monoclonal antibody against human ITGB1. DKK1 was used as negative control. Nuclei were counterstained with DAPI(blue) and the actin filaments with Phalloidin (red) Scalebar is 10 μ m, objective 20x.

The FSH-14F8 and Bi14F8 show binding in the focal adhesions. Cells can adhere to for example a fibronectin substrate via the integrin $\alpha 5\beta 1$, present in focal adhesions.⁵² The binding of FSH-14F8 and Bi14F8 seem to target the integrins in the focal adhesions and might therefore influence the cell-matrix interaction. To determine if the binding and spreading of living cells in culture is influenced by 14F8, the influence of VHH binding on cell adherence to the matrix was determined, which is explained in chapter 3.3.

To determine the binding efficiency of BMP-7 to the bispecific VHHs in the third immunofluorescence experiment, the VHHs were first pre-incubated with BMP-7 before being added to the fixated cells. The staining pattern is comparable with the previous experiment that showed localization of the binding of VHHs towards the ITGB1 receptor. The result is shown in figure 7. These results confirm that BMP-7 can be loaded onto the bispecific VHH carrier system. In addition, BMP-7 can be stained with a secondary antibody while bound to the VHH, presumably indicating that the growth factor maintains its active conformation.

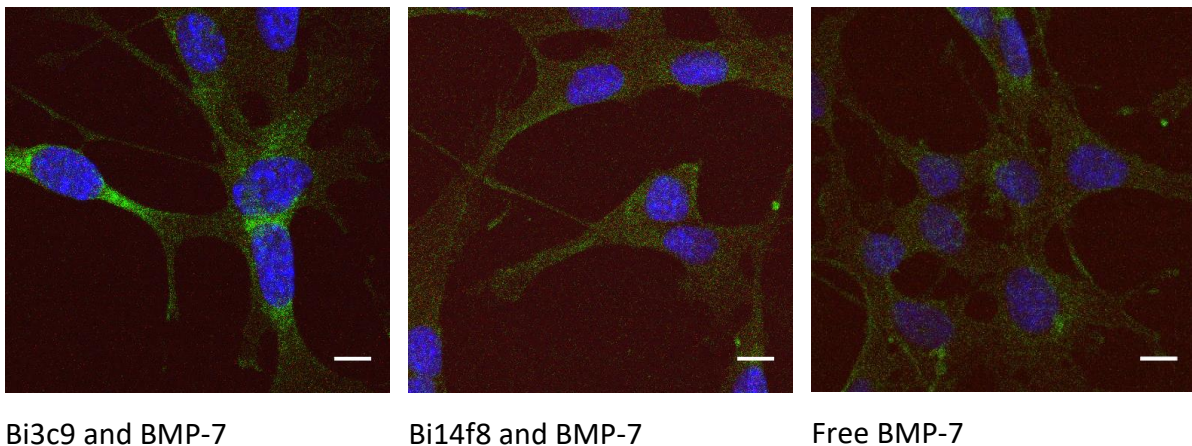


Figure 7: Staining of BMP-7 bound to VHH carrier system on fixed C2C12 BRE-Luc cells. Cells were adhered to cover slides, fixed with formaldehyde, and incubated with VHH pre-incubated with BMP-7 as indicated in the figure, as primary antibodies. VHH were detected by a secondary antibody coupled to Alexa Fluor 488 (green). Nuclei were counterstained with DAPI (blue) and the actin filaments with Phalloidin (red). Scale bar is 10 μm , objective 20x.

3.3 Functionality assays

Influence of VHHs on matrix-cell interaction

In chapter 3.2 it became clear that the binding of FSH-14F8 and Bi14F8 is localized near the focal adhesions. To assess if the binding of the VHHs interferes with the adherence of the cell to the matrix, the influence of VHHs on the cell-matrix interaction was determined. The results are shown in figure 8. To visualize the spreading of cells, the circularity of the cells was measured as a value from 0 to 1. A value closer to 1 represents a more circular shape of the cell.

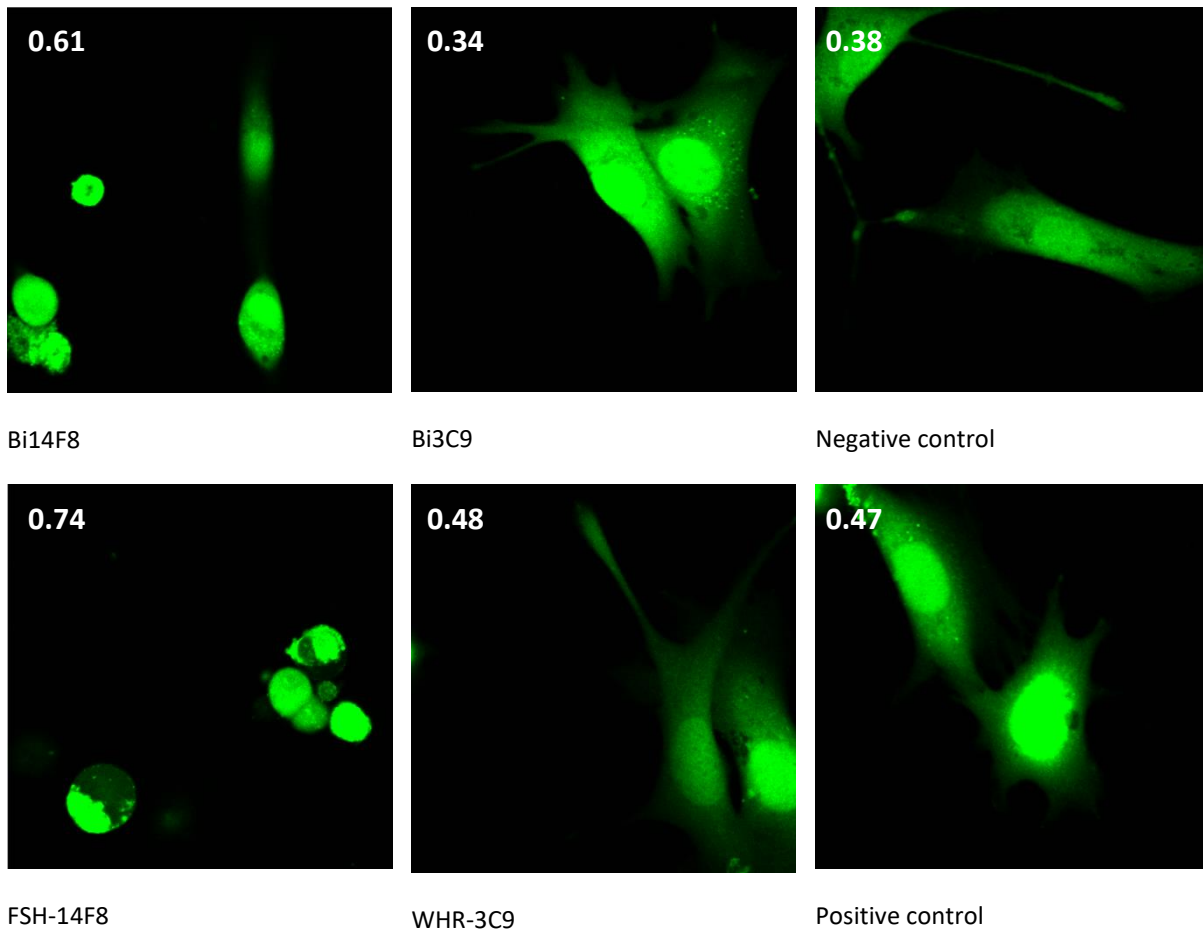


Figure 8: Influence of incubation with 100 nM VHHs, the positive control and the negative control, on adherence of C2C12 BRE-Luc cells after 24 hours. The circularity of C2C12 BRE-Luc cells is shown as a value between zero and one, depicted together with the corresponding fluorescent image. A value closer to one represents a higher influence of the VHH on cell adherence and is an average of 2 images obtained with a 20x objective.

Indeed, mono- and Bi14F8 were able to inhibit binding of C2C12 BRE-Luc cells to a greater extent after one day of culture, when compared to mono- and Bi3C9. The value of 3C9 is similar to the negative control. The positive control (mouse monoclonal antibody against human ITGB1) showed no inhibition of binding. This result is in line with the immunofluorescent assay, where no binding of the positive control was observed.

Luciferase assay

To determine if the bound BMP-7 on the VHHs was able to initiate signal transduction on C2C12 BRE-Luc cells, the luciferase reporter assay was performed. The effect of the anti-BMP-7 VHH on BMP-7 can be described as binding (non-neutralizing), blocking or neutralizing and was determined in this luciferase assay.

First, the optimal BMP-7 concentration to measure an upregulation of the BMP responsive gene was determined. The optimization of the luciferase assay showed upregulation of BRE-

Luc expression after 14 hours of BMP-7 stimulation in a dose-dependent manner, with a significant upregulation for BMP-7 concentrations of 10 and 100 ng/ml of 15.0 and 70.3 times respectively, shown in figure 1 of the supplementary data.⁵³ Based on this result, the concentration of 10 ng/ml BMP-7 was used in the first luciferase reporter assay with incubation of BMP-7 in presence or absence of VHH.

In figure 9, the results of this experiment are displayed. BMP-7 treatment resulted in a 4.7 fold increase in reporter activity compared to the negative control. The VHHs were added equimolar with BMP-7, and in 10 and 100 times excess. The bispecific VHHs have a significantly lower expression level compared to the negative control. This is in line with the high binding affinity towards BMP-7, measured in the SPRi experiment described before. Only the stimulation with equimolar BI3C9 and BMP-7, both with and without pre-incubation, show a significant upregulation compared to the negative control. However, these conditions show both an increase of 1.7 compared to the negative control, whereas free BMP-7 stimulation results in a 4.7 fold increase of BRE-Luc expression.

In this first luciferase reporter assay, both BI14F8 and BI3C9 show a neutralizing effect, since an excess of VHH results in a lower BRE-Luc expression. Therefore the affinity of BMP-7 is higher for VHHs compared to the cell receptor. To determine if BMP-7 is released over time, the second luciferase assay was performed.

To verify if the VHHs can be used for a long term release system, the luciferase assay was adapted by incubating the VHH and BMP-7 consecutively for several time points. The hypothesis was, that over time BMP-7 was released from the VHH. Two main conditions were taken into account, VHH in molar excess of BMP-7 and an equimolar amount of VHH with BMP-7. It was expected that over time the difference between these two conditions was decreased as BMP-7 releases from the VHH, resulting in a similar luciferase response.

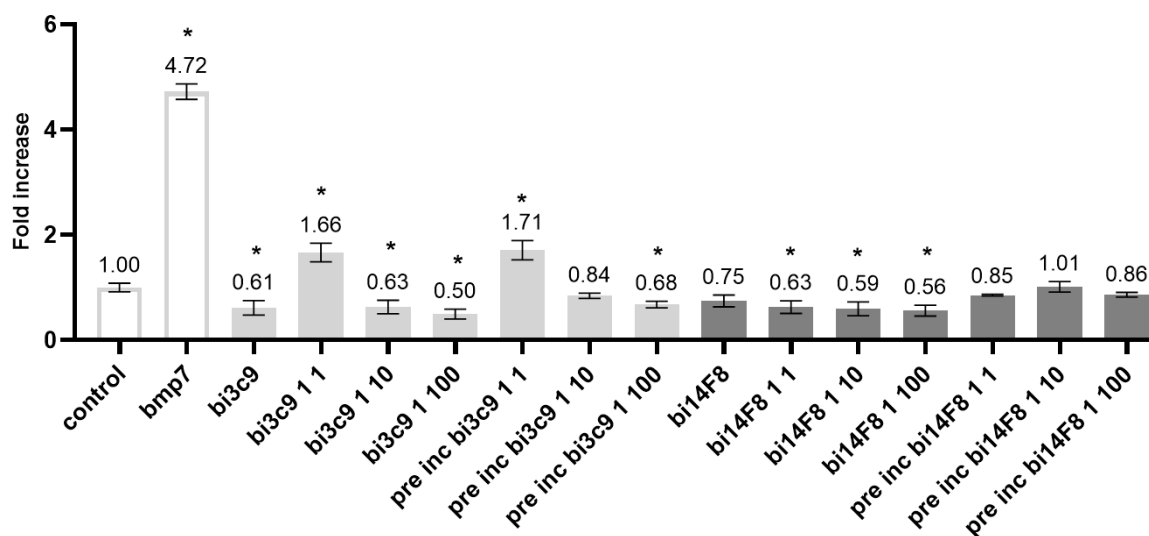


Figure 9: Relative BRE-Luc expression after 14 hours of stimulation in C2C12 BRE-Luc cells. The results are normalized to the negative control. * = $p < 0.05$ compared to the negative control. N = 4

Figure 10 shows a distinct difference from the previous assay, comparing the equimolar VHH and BMP-7 conditions with free BMP-7. The fold increase of Bi3C9 with equimolar BMP-7 is comparable to free BMP-7. Bi14F8 shows a significant increase compared to the negative control whereas in the previous experiment this was not the case. Comparing both VHHs, it is obvious that after 14 hours Bi3C9 results in a higher upregulation of BRE-Luc.

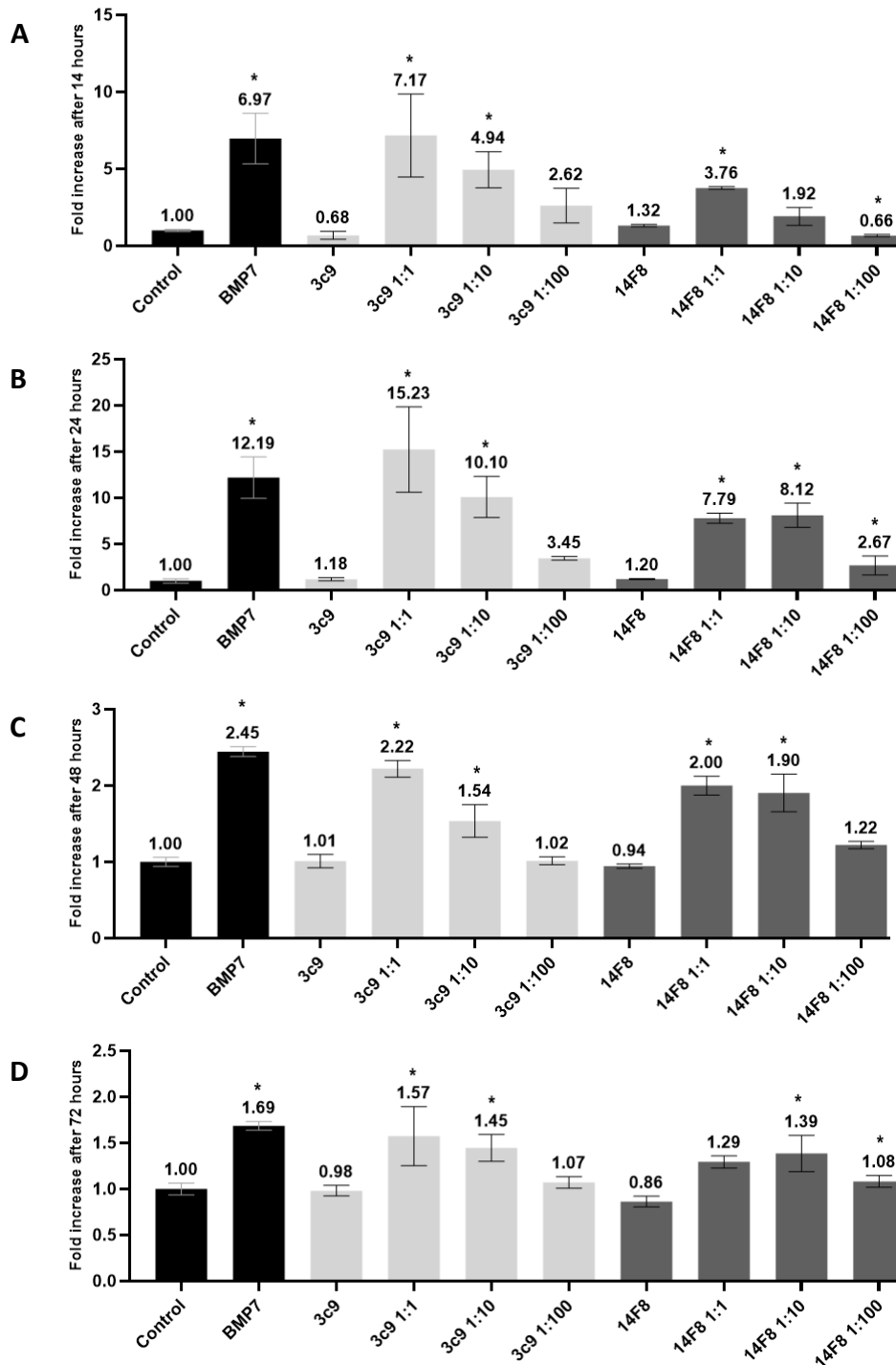


Figure 10: Relative BRE-Luc expression after stimulation with BMP-7 in presence or absence of bispecific VHHs in C2C12 BRE-Luc cells for A) 14 hours, B) 24 hours, C) 48 hours, and D) 72 hours. The results are normalized to the negative control. * = $p < 0.05$ compared to the negative control. N = 4

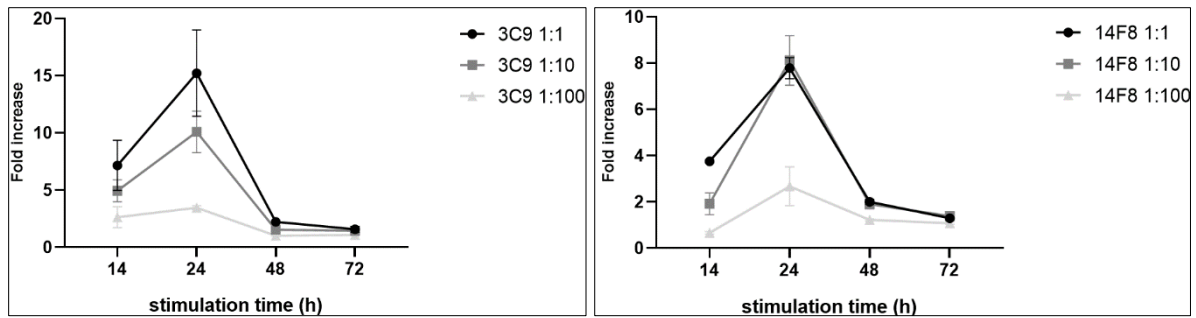


Figure 11: Fold increase of BRE-Luc expression after 14, 24, 48, and 72 hours, comparing equimolar VHH and BMP-7 with VHH added in excess.

It is worth mentioning that after 48 and 72 hours, the activation of free BMP-7 decreased to values of 2.5 and 1.7 respectively. Furthermore, it is important to point out that cell growth was observed after 48 and 72 hours of stimulation in all conditions. For reliable results, this experiment needs to be repeated with a lower concentration of FBS to ensure proper starvation of the cells.

Nevertheless, some promising observations can be made from this experiment. The most remarkable result is the reducing difference over time when comparing the VHHs with equimolar BMP-7 and the conditions with VHH added in excess 1:10 and 1:100. To highlight this effect, the fold increase values of all concentrations VHHs incubated with BMP-7 over time, were summarized in figure 11. It is evident for both VHHs that the difference in fold change decreases after 48 hours of stimulation, especially the conditions 10 times excess (1:10) and equimolar VHH with BMP-7 (1:1). From this experiment, it can be assumed that BMP-7 is released from the VHH over time.

3.4 Pathway activation

qPCR

The inhibitor of Differentiation 1 (Id1) is a primary target gene in the Smad signaling pathway. To verify whether the BMP signaling pathway is activated by BMP-7 in C-20/A4 cells and to determine the influence of VHHs on this, the effect of BMP-7 on the expression of the primary BMP target gene Id1 was measured.

The expression of the markers TCF1, LEF1, SOX9, Runx2, B2M, and Id1 was tested. The hypothesis was, that BMP-7 stimulation was going to result in upregulation of the direct target gene Id1 and the indirect target genes TCF1, LEF1, and SOX9.^{54,55} Furthermore, the expression of the marker for hypertrophic differentiation Runx2 was measured.

All stimulated conditions remained the same for markers TCF1, LEF1, SOX9 and Runx2 after stimulation for 6 and 24 hours, shown in figure 2 of the supplementary data. This upregulation might still occur after stimulation for longer times. For this study, determination of upregulation by BMP-7 of the indirect markers TCF1, LEF1 and SOX9 was not the aim and will not be studied, because Id1 showed upregulation after BMP-7 stimulation, as expected.

Stimulation of the cells with BMP-7 significantly increased the Id1 expression using free BMP-7 compared to the untreated control with a maximum increase of 12.2-fold after 6 hours and 13.6 after 24 hours, shown in figure 12. Evaluating all other conditions, only stimulation with equimolar Bi3C9 and BMP-7 after 6 hours significantly increased the expression of Id1 compared to the negative control with a fold increase of 6.5.

This result is in line with the luciferase reporter assay shown in figure 5 where all conditions showed a significantly lower signal compared to free BMP-7. Comparing the bispecific VHHs to the negative control, no significant difference was measured and therefore the same neutralizing effect as shown in the luciferase assay was observed in this cell type. Consequently, the primers for Id1 can be used for future experiments on human chondrocytes to show a possible effect after BMP-7 stimulation.

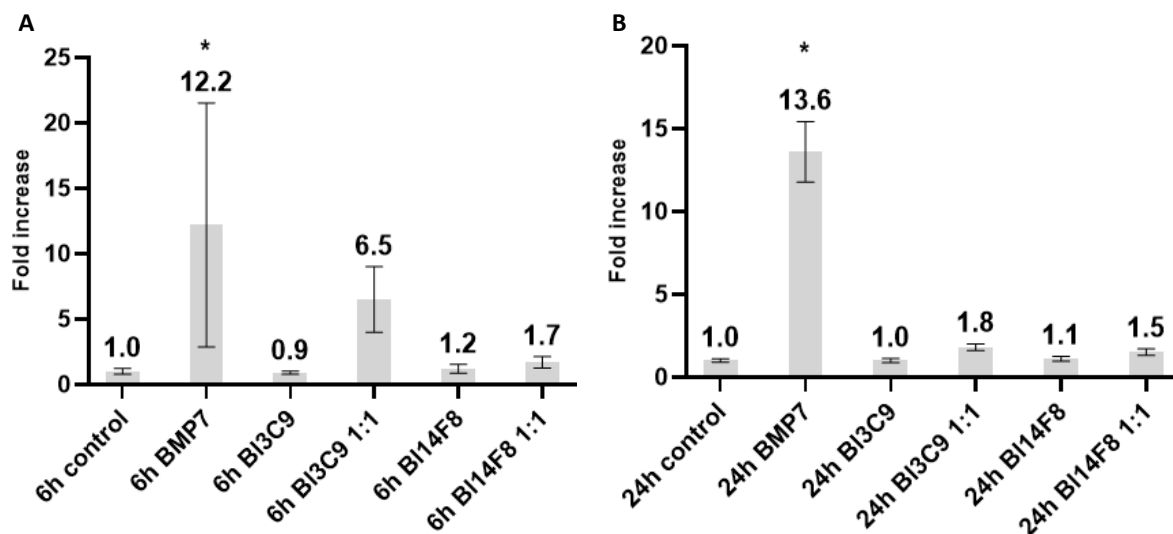


Figure 12: Gene expression of Id1 after stimulation with BMP-7, Bi3C9, Bi14F8, or an equimolar mixture of BMP-7 with bispecific VHHs. qPCR results are normalized to B2M. Data were expressed as fold change compared to the unstimulated control. A) 6 hours of stimulation. B) 24 hours of stimulation. * p < 0.05 compared to the negative control.

Western blot

To assess the effect of BMP-7 stimulation on the protein level, Smad1/5/8 phosphorylation was determined with a western blot assay. To determine if the binding of VHHs to the ITGB1 receptor results in phosphorylation, FAK was tested. It is important to decide if

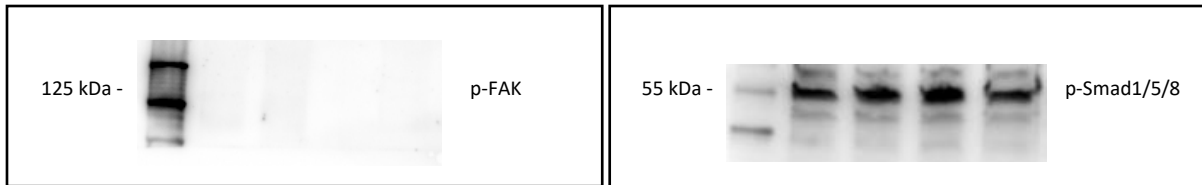


Figure 13: Explanatory western blot data, after stimulation simultaneously with the qPCR experiment (BMP-7 in the presence or absence of bispecific VHHs and the negative control) resulted in no phosphorylation from FAK and an unquantifiable signal of p-Smad1/5/8 due to the drying out of the membrane during antibody incubation.

phosphorylation is absent to be able to use ITGB1 as a decoy receptor in this proof of principle study. The first western blot was performed simultaneously with the qPCR experiment. The cells were stimulated with BMP-7 in the presence or absence of bispecific VHHs and the negative control. The membranes were dried out after the incubation with the first antibody due to power failure. However, it was clear that FAK was not phosphorylated, shown in figure 13. Phosphorylated p-Smad1/5/8 could not be quantified, since the membrane dried out during antibody incubation, which made it impossible to stain for Smad1/5/8.

After this experiment, it was decided to first test the effect of stimulation with free BMP-7 on Smad1/5/8 phosphorylation after 15, 30, 60, and 120 minutes. This experiment was successfully conducted on 2 membranes and membrane 1 is shown in figure 14. There is no clear difference visible by observing the different incubation times in this figure.

The intensity of the bands was analyzed with ImageJ. The results are shown in Table 4 of the supplementary data. Beta-actin values were determined to see if an equal amount of protein was loaded in the slots of the gel. Considering the fact that the same membrane was used to stain for phosphorylated and normal Smad1/5/8, beta Actin is not needed for normalizing.

The ratio p-Smad1/5/8 to total Smad1/5/8 was calculated and shown in table 1. Since the difference in intensity is not visible by observing figure 14 and the results shown in table 1 are conflicting, the experiment has to be repeated for reliable results. Furthermore, a concentration range of BMP-7 has to be analyzed to be able to see clear differences in phosphorylation between the incubation time points.

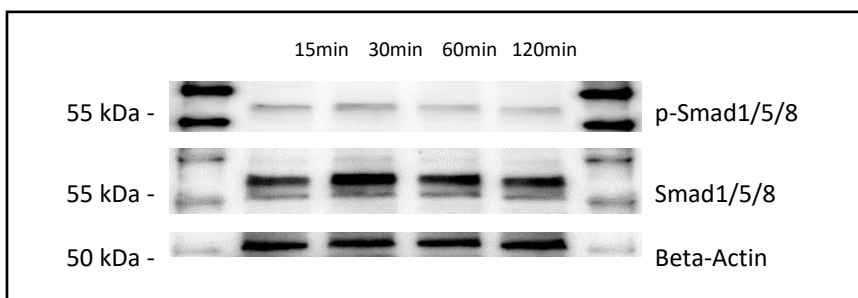


Figure 14: Western blot of membrane 1 after stimulation with 40 ng/ml BMP-7 for 15, 30, 60 and 120 minutes. Phosphorylated Smad1/5/8, normal Smad1/5/8 and beta actin for normalization.

Table 1: The calculated ratio p-Smad1/5/8 to total Smad1/5/8 of the two membranes, stimulated with 40 ng/ml BMP-7 for 15, 30, 60, and 120 minutes.

Time (minutes)	Membrane 1	Membrane 2
15	1.27	0.81
30	1.04	1.08
60	0.88	1.32
120	0.83	0.84

4. Discussion

At the moment, there are no disease-modifying treatments available for OA. This research evaluated whether it is possible to influence the BMP pathway in chondrocytes with BMP-7 delivery. To target chondrocytes *in vitro*, bispecific VHHs that bind both the cell adhesion receptor ITGB1 and BMP-7 can act as a concentrator for BMP-7 to facilitate sustained release.

To determine whether VHH can be used for the targeted delivery of BMP-7, several experiments were designed and the results will be discussed in this chapter. SPRi measurements showed a high binding affinity of both bispecific VHHs for ITGB1 and BMP-7. The binding of the VHHs to ITGB1 was visualized with immunofluorescence to determine the subcellular location and showed binding of FSH-14F8 and Bi14F8 near the focal adhesion. Incubation with FSH-14F8 and Bi14F8 resulted in less stretching of the cell, whereas WHR-3C9 and Bi3C9 showed no effect on cell adhesion. The bifunctional VHHs showed a neutralizing effect in the first luciferase assay and the qPCR analysis. The data of the final luciferase assay suggest that the VHHs are suitable for targeted drug delivery in this proof of principle study because longer incubation periods showed the release of BMP-7 from the VHH. In this section, all findings will be discussed and compared with other studies.

Characterization

As stated in the results section, biphasic fitting was used to process the SPRi measurements. Although the biphasic curves are fitted nicely as shown in the supplementary data, table s2 and s3, it is recommended to optimize the experimental parameters by lowering the ligand density and the analyte concentration.⁵⁶ Examples of potential sources of this type of biphasic interaction are the random immobilization of the amine coupling, impure ligand, or analyte. Furthermore, it is recommended to use a ligand density that results in an analyte response below 100 Response Units (RU).⁵⁶ It should be mentioned that a Bi3C9 ligand concentration of 128 nM shows a deviant binding affinity value for BMP-7 analyte of 914.6, comparing to ligand concentrations of 256 and 64 nM, where a K_D of 98.88 and 184 nM respectively was measured. The ligand Bi3C9 with a concentration of 128 nM resulted in 40 as the highest RU response, whereas a concentration of 64 nM resulted in a higher overall response. For reliable results, this measurement has to be repeated. Comparing the binding affinity of the VHHs towards BMP-7, Bi14F8 seems to have a lower K_D value and therefore a higher binding affinity.

Previous studies showed an affinity of 20 nM for BMP-7 towards type I BMPRs. It has a greater affinity for the type II receptors as it binds to BMPR-II and ACTR-IIB with a K_D of 6 nM, and with an even greater affinity of 1.3 nM to ACTR-IIA.⁵⁷ Since these values were determined with a different technique, the experiment has to be repeated to be able to compare the affinity of BMP-7 for the receptor and the bifunctional VHHs. However, when comparing the results from

Khodr et al. with this study, BMP-7 has a higher binding affinity for the cell surface receptors compared to the VHHs. For this study, the most important observation is that both VHHs show a high affinity for ITGB1 and BMP-7. The VHHs are therefore suited for targeted delivery in this proof of principle study. The release of BMP-7 was analyzed in the subsequent experiments.

Localization

The results of the immunofluorescent experiment indicate a different binding location when comparing the two VHH clones 14F8 and 3C9. Although the staining suggests that FSH-14F8 and Bi14F8 can influence the binding of the cells to the matrix, the western blot data does not show phosphorylation of FAK, indicating that a decoy receptor is targeted.

The VHHs were genetically fused in a bispecific VHH using a flexible amino acid GS linker (Gly and Ser residues). GS linkers have been shown to improve folding and stability in fusion protein examples.^{58,59} We showed in the immunofluorescent experiment, that the bispecific construction of the VHH did not affect the binding to either epitope. These findings confirm that both VHHs can be used in this proof of principle study to target ITGB1 as a decoy receptor *in vitro*.

It should be noted that the binding of FSH-14F8 and Bi14F8 result in limited attachment of the cells. Integrins-based adhesion sites connect the F-actin cytoskeleton of cells to the ECM and transduce mechanical forces, whereupon biochemical signals can be induced that are able to regulate rapid responses in cellular mechanics and long-term changes in gene expression.^{60,61} The binding of 14F8 can therefore play a role in tissue homeostasis and should be taken into account. Liang et al. stated, that periodic mechanical stress promotes chondrocyte proliferation and matrix synthesis.⁶² For future experiments, it should be taken into account that incubation with 14F8 can influence binding and therefore decrease mechanical stress exerted on the chondrocytes.

Cell viability assays such as MTT and Alamar blue can be used to determine if the cells have an active metabolism after incubation with the VHHs.⁶³ In this way, the possible effect of reduced mechanical stress by binding of FSH-14F8 and Bi14F8 can be assessed by measuring and comparing the metabolic activity of treated cells with the negative control. The MTT assay is an endpoint measurement because of its cytotoxicity and should be performed simultaneously in future luciferase and qPCR experiment.

The mouse monoclonal antibody against human ITGB1 was used as a positive control in the immunofluorescent assays. Although there is a high resemblance between mice and human ITGB1 of 92.5%, the staining in the positive control was absent in the immortalized mouse myoblast cell line C2C12. Loeser et al. showed expression of the ITGB1 subunit (CD29) on C-20/A4 using flow cytometry.⁶⁴ Given the fact that the staining is negative in both C2C12 cells

and the human chondrocyte cell line C-20/A4, the antibody was most probably of older age and a new batch has to be purchased for future experiments.

Pathway activation

The BMP responsive C2C12 BRE-Luc mouse muscle myoblast cell line was stimulated with BMP-7 in presence or absence of VHH as described in the results and evaluated for an increase in BRE-Luc activation compared to the negative control. The first luciferase assay aimed to determine the effect of the VHHs on BMP-7 delivery. An increase in activation of BRE-Luc was observed in equimolar Bi3C9 and BMP-7. All other conditions in presence of VHH showed neutralization. For future experiments, a modified anti-BMP-7 VHH can be produced to lower the binding affinity for BMP-7, resulting in a shift of the dynamic balance as depicted in figure 15. This can be achieved by modifying the BMP7-G7 VHH by replacing amino acids in the domain that influences binding. This might decrease the K_D of the VHH towards BMP-7, solving the neutralizing effect of the VHH. In this way, an optimal balance between BMPR and anti-BMP-7 VHH can be achieved.

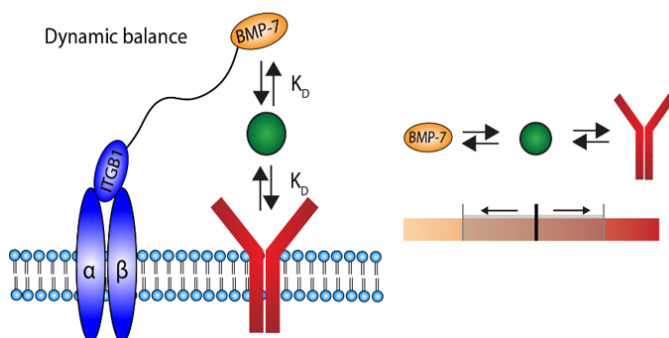


Figure 15: Dynamic balance between the binding affinity of BMP-7 towards BMP7-G7 and the cell surface receptor to enable the delivery of BMP-7 to the cells.

The second luciferase assay showed a different activation pattern, comparing free BMP-7 and BMP-7 in presence of bispecific VHHs. This pattern can be explained by the subsequent adding of VHH and BMP-7 instead of adding a mixture of both, preventing unbound BMP-7 to be present in solution. These higher levels of the BMP responsive element indicate binding of the growth factor to both the VHH and the BMPR.

In agreement with the first assay, Bi3C9 showed a higher upregulation compared to Bi14F8. One plausible reason is the binding pattern, shown in the immunofluorescence assays. Here, a diffuse binding pattern was shown for Bi3C9, resulting in more binding possibilities for the bispecific VHHs and BMP-7, resulting in a higher level of BRE-Luc expression.

Important to note is the decrease in expression level of free BMP-7 after 48 and 72 hours. Previous studies showed a maximal upregulation of BRE-Luc after 15 hours, followed by a decrease in signal after 12 hours.⁵³ A possible explanation for the measured 12.19 fold upregulation after 24 hours in comparison with a value of 6.97 after 14 hours, is the observed cell growth over time. The consequence of this cell growth is more available type II receptors compared to the first time point of 14 hours, possibly resulting in the higher upregulation after 24 hours. Starvation medium with 1% FBS was chosen based on previous experiments and optimization in this research group. The findings in this study suggest a lower FBS concentration is required to ensure cell cycle arrest.

The expression of the Smad target gene ID-1 upon stimulation with BMP-7 in presence or absence of VHH in C-20/A4 cells was examined using qPCR. The aim was to determine if a similar neutralizing effect was observed, which was the case in the first luciferase experiment. Only equimolar Bi3C9 with BMP-7 resulted in upregulation compared to the negative control.

For further analysis, the efficacy of long term delivery using VHHs as a delivery system should be verified for this cell type. The optimal stimulation time needs to be determined, using the same experimental set-up with incubation of VHH and BMP-7 consecutively as described in the second luciferase experiment. To determine if the stimulation, resulting in Id-1 expression at the gene level, is translated to actual protein synthesis, western blot experiments or qPCR analysis could be used to determine the anabolic activity of chondrocytes. For example, type II collagen production could be determined.⁶⁵ In this study, a human chondrocyte cell line was used to determine the effect of BMP-7 stimulation, in presence or absence of VHHs. Previous studies showed upregulation after BMP-7 stimulation of anabolic markers collagen type II and aggrecan, and a decrease in catabolic markers MMP 1, 3 and 13 in OA primary human chondrocytes.⁶⁶ To determine the effect of BMP-7 stimulation on human primary chondrocytes, stimulation of this cell type has to be compared to the results with C-20/A4 cells.

Western blot experiments were performed to decide the effect of BMP-7 stimulation on phosphorylation of Smad, on a protein level. However, no differences were observed between the four incubation times. To see if SMAD is phosphorylated in a dose-dependent manner, a concentration range of BMP-7 has to be tested. In the experiment described in this study, only one incubation concentration is analyzed. According to Klatte-Schulz et al. BMP-7 induced phosphorylation of Smad 1/5/8 after 30 and 60 minutes of stimulation in human tenocyte-like cells, where two different BMP-7 concentrations were used to show upregulation of the signal. It should be noted that the western blot analysis does not enable the determination of long term release effects, since this assay shows upregulation of phosphorylated Smad 1/5/8 after a maximum incubation of two hours. Therefore, qPCR experiments are more suitable to determine the effect of BMP-7 stimulation on the pathway activation of chondrocytes.

5. Conclusion

In conclusion, it was shown that both bifunctional VHHs can be exploited for long term BMP-7 delivery. The findings clearly indicate that Bi3C9 showed less impact on the spreading of cells and a higher upregulation of the BMP responsive gene compared to Bi14F8. This paper suggests that Bi3C9 showed beneficial characteristics and should be used in further *in vitro* experiments. This study has clearly shown that bispecific VHHs can be used for targeted delivery of BMP-7 *in vitro* and shows great promise for disease-modifying treatment for the regeneration of cartilage.

6. Future perspectives

Since the experiments were conducted on cultured cells *in vitro*, ITGB1 was chosen as a target to show the effect of BMP-7 stimulation in 2D cell culture. This study mainly focuses on the ability of BMP7-G7 to deliver and release BMP-7. For future experiments *in vivo*, a VHH that specifically targets chondrocytes is required and needs to be characterized. Hydroxyapatite is a crystal present in the superficial and deep layers of the cartilage, as well as in synovial fluid and the meniscus.^{67,68} This target was used in a previous study and the bispecific VHH demonstrated successful targeting and accumulation in bone, targeting BMP-7 and hydroxyapatite.⁴⁰ This study by Huang et al. showed the functionality of BMP7-G7 *in vivo*.

To specifically target chondrocytes *in vivo* in future experiments, the ITGB1 binding part of the bispecific VHHs has to be replaced by a chondrocyte specific protein. Matrilin-3 is found almost exclusively in cartilage and plays a role as a linker molecule in the network of the articular cartilage.⁶⁹ Upper zone of growth plate and Cartilage Matrix Associated protein (UCMA) has been reported as cartilage-specific secreted protein and suggested to be a negative regulator of osteogenic differentiation in mice.^{69,70}

The two most promising targets for *in vivo* purposes are Cartilage Intermediate Layer Protein-1 (CILP-1) which is thought to play a role in cartilage scaffolding and Cartilage Oligomeric Matrix Protein (COMP) which has been suggested to be upregulated either to repair damage or slow matrix breakdown during the late stages of OA.⁷¹ The molecular organization of ECM is shown in figure 16.

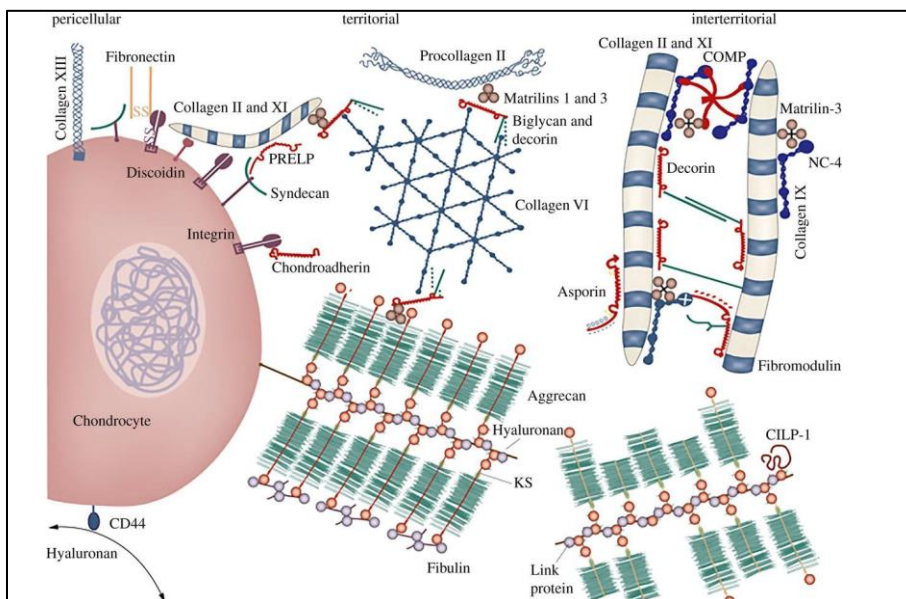


Figure 16: The molecular organization of ECM in articular cartilage. The chondrocyte is surrounded by pericellular matrix, where molecules interact with cell surface receptors. Next to the pericellular matrix, slightly further from the cell, lies the territorial matrix. At the largest distance from the cell is the interterritorial matrix.⁷²

In OA, complexes of COMP are removed from the interterritorial matrix and found in the synovial fluid of patients, while at the same time new synthesis of the molecule results in deposition primarily in the pericellular matrix of the cartilage.^{69,72} Massive new accumulation close to the cells is also observed for CILP-1. The change of distribution pattern of COMP and CILP-1 are a promising target for OA. Research will show if delivery of BMP-7 is efficient and whether or not the cells can be stimulated when targeting CILP-1 or COMP.

Osteochondral platform

To model the structure and biology of the joint *in vitro*, a three-dimensional model can be used in future experiments, to investigate targeting and delivery functioning of the bifunctional VHHs.⁷³ This osteochondral platform can be used to determine tissue penetration by labeling of the VHHs and pathway activation can be monitored by performing qPCR experiments as described in this discussion. Furthermore, matrix production after BMP-7 stimulation can be assessed by e.g. immunohistochemical staining of collagen type II after paraffin embedding and cross-sectioning. For real-time monitoring, a Dimethylmethylene Blue Assay (DMMB) could be performed to determine the glycosaminoglycan (GAG) concentration in the culture medium.^{74,75}

7. Bibliography

1. Allen, K. & Golightly, Y. M. Epidemiology of osteoarthritis: state of the evidence. *Curr Opin Rheumatol* **27**, 276–283 (2015).
2. Hunter, D. J. & Bierma-Zeinstra, S. Osteoarthritis. *Lancet* **393**, 1745–1759 (2019).
3. Kloppenburg, M. & Berenbaum, F. Osteoarthritis year in review 2019: epidemiology and therapy. *Osteoarthr. Cartil.* **28**, 242–248 (2020).
4. Bannuru, R. R. *et al.* OARSI guidelines for the non-surgical management of knee, hip, and polyarticular osteoarthritis. *Osteoarthr. Cartil.* **27**, 1578–1589 (2019).
5. Yu, S. P. & Hunter, D. J. Intra-articular therapies for osteoarthritis. *Expert Opin. Pharmacother.* **17**, 2057–2071 (2016).
6. Thysen, S., Luyten, F. P. & Lories, R. J. U. Targets, models and challenges in osteoarthritis research. *DMM Dis. Model. Mech.* **8**, 17–30 (2015).
7. Martel-Pelletier, J. *et al.* Osteoarthritis. *Nat. Rev. Dis. Prim.* **2**, (2016).
8. Goldring, S. R. & Goldring, M. B. Changes in the osteochondral unit during osteoarthritis: Structure, function and cartilage bone crosstalk. *Nat. Rev. Rheumatol.* **12**, 632–644 (2016).
9. Deng, Z. H., Li, Y. S., Gao, X., Lei, G. H. & Huard, J. Bone morphogenetic proteins for articular cartilage regeneration. *Osteoarthr. Cartil.* **26**, 1153–1161 (2018).
10. Fassbender, H. G. Role of chondrocytes in the development of osteoarthritis. *Am. J. Med.* **83**, 17–24 (1987).
11. Man, G. S. & Mologhianu, G. Osteoarthritis pathogenesis - a complex process that involves the entire joint. *J. Med. Life* **7**, 37–41 (2014).
12. Eyre, D. R. Collagens and cartilage matrix homeostasis. *Clin. Orthop. Relat. Res.* 118–122 (2004). doi:10.1097/01.blo.0000144855.48640.b9
13. Wang, M. *et al.* MMP13 is a critical target gene during the progression of osteoarthritis. *Arthritis Res. Ther.* **15**, 1–11 (2013).
14. Heijink, A. *et al.* Biomechanical considerations in the pathogenesis of osteoarthritis of the knee. *Knee Surgery, Sport. Traumatol. Arthrosc.* **20**, 423–435 (2012).
15. Nam, J. *et al.* Sequential alterations in catabolic and anabolic gene expression parallel pathological changes during progression of monoiodoacetate-induced arthritis. *PLoS One* **6**, (2011).
16. Zhang, W., Robertson, W. B., Zhao, J., Chen, W. & Xu, J. Emerging trend in the pharmacotherapy of osteoarthritis. *Front. Endocrinol. (Lausanne)*. **10**, (2019).
17. Pei, M. & He, F. Extracellular matrix deposited by synovium-derived stem cells delays replicative senescent chondrocyte dedifferentiation and enhances redifferentiation. *J. Cell. Physiol.* **227**, 2163–2174 (2012).
18. Shi, S., Chan, A. G., Mercer, S., Eckert, G. J. & Trippel, S. B. Endogenous versus Exogenous Growth Factor Regulation of Articular Chondrocytes Shuiliang. *J Orthop Res.* **32**, 1–7 (2014).

19. Gavenis, K., Heussen, N. & Schmidt-Rohlfing, B. Effects of low concentration BMP-7 on human osteoarthritic chondrocytes: Comparison of different applications. *J. Biomater. Appl.* **26**, 845–859 (2012).
20. Gavenis, K., Schneider, U., Groll, J. & Schmidt-Rohlfing, B. BMP-7-loaded PGLA microspheres as a new delivery system for the cultivation of human chondrocytes in a collagen type I gel: The common nude mouse model. *Int. J. Artif. Organs* **33**, 45–53 (2010).
21. Chubinskaya, S. & Kuettner, K. E. Regulation of osteogenic proteins by chondrocytes. *International Journal of Biochemistry and Cell Biology* **35**, 1323–1340 (2003).
22. Nishida, Y., Knudson, C. B., Kuettner, K. E. & Knudson, W. Osteogenic protein-1 promotes the synthesis and retention of extracellular matrix within bovine articular cartilage and chondrocyte cultures. *Osteoarthr. Cartil.* **8**, 127–136 (2000).
23. Nishida, Y., Knudson, C. B., Eger, W., Kuettner, K. E. & Knudson, W. Osteogenic protein 1 stimulates cell-associated matrix assembly by normal human articular chondrocytes: Up-regulation of hyaluronan synthase, CD44, and aggrecan. *Arthritis Rheum.* **43**, 206–214 (2000).
24. Hunter, D. J. *et al.* Phase 1 safety and tolerability study of BMP-7 in symptomatic knee osteoarthritis. *BMC Musculoskelet. Disord.* **11**, 232 (2010).
25. Hayashi, M. *et al.* Intra-articular injections of bone morphogenetic protein-7 retard progression of existing cartilage degeneration. *J. Orthop. Res.* **28**, 1502–1506 (2010).
26. Gautschi, O. P., Frey, S. P. & Zellweger, R. Bone morphogenetic proteins in clinical applications. *ANZ J. Surg.* **77**, 626–631 (2007).
27. Horbelt, D., Denkis, A. & Knaus, P. A portrait of Transforming Growth Factor β superfamily signalling: Background matters. *Int. J. Biochem. Cell Biol.* **44**, 469–474 (2012).
28. Wang, R. N. *et al.* Bone Morphogenetic Protein (BMP) signaling in development and human diseases. *Genes Dis.* **1**, 87–105 (2014).
29. Cecchi, S., Bennet, S. J. & Arora, M. Bone morphogenetic protein-7: Review of signalling and efficacy in fracture healing. *J. Orthop. Transl.* **4**, 28–34 (2016).
30. Jeong, J. W. *et al.* ID1-mediated bmp signaling pathway potentiates glucagon-like peptide-1 secretion in response to nutrient replenishment. *Int. J. Mol. Sci.* **21**, 1–13 (2020).
31. Chubinskaya, S. Identification of ID proteins in human articular cartilage and the effect of growth factors on their expression. in
32. Wang, Z. *et al.* Novel biomaterial strategies for controlled growth factor delivery for biomedical applications. *NPG Asia Mater.* **9**, e435-17 (2017).
33. Koerselman, M., Huang, X., Rodrigues, E. D., Verrips, T. & Karperien, M. Heterospecific bivalent heavy chain only antibodies for targeting BMP7 to osteochondral lesions. *Osteoarthr. Cartil.* **27**, S436–S437 (2019).
34. Wang, Y., Newman, M. R. & Benoit, D. S. W. Development of controlled drug delivery systems for bone fracture-targeted therapeutic delivery: A review. *Eur. J. Pharm.*

- Biopharm.* **127**, 223–236 (2018).
35. Koria, P. Delivery of growth factors for tissue regeneration and wound healing. *BioDrugs* **26**, 163–175 (2012).
 36. Vincke, C. & Muyldermans, S. Introduction to Heavy Chain Antibodies and Derived Nanobodies. *Methods Mol Biol* **911**, 65–78 (2012).
 37. Muyldermans, S. Nanobodies: Natural Single-Domain Antibodies. *Annu. Rev. Biochem.* **82**, 775–797 (2013).
 38. Press, D. Bispecific antibodies : design , therapy , perspectives. *Drug Des. Devel. Ther.* **12**, 195–208 (2018).
 39. Smolarek, D., Bertrand, O. & Czerwinski, M. Variable fragments of heavy chain antibodies (VHHs): A new magic bullet molecule of medicine? *Postepy Hig. Med. Dosw.* **66**, 348–358 (2012).
 40. Huang, X. *Multi-Signals Involved in Human Joint Homeostasis.* (2018).
 41. Howe, G. A. & Addison, C. L. β 1 integrin. *Cell Adh. Migr.* **6**, 71–77 (2012).
 42. Lian, C. *et al.* Collagen type II suppresses articular chondrocyte hypertrophy and osteoarthritis progression by promoting integrin β 1–SMAD1 interaction. *Bone Res.* **7**, (2019).
 43. Hendriks, J., Stojanovic, I., Schasfoort, R. B. M., Saris, D. B. F. & Karperien, M. Nanoparticle Enhancement Cascade for Sensitive Multiplex Measurements of Biomarkers in Complex Fluids with Surface Plasmon Resonance Imaging. *Anal. Chem.* **90**, 6563–6571 (2018).
 44. Schasfoort, R. B. M. *et al.* Interpolation method for accurate affinity ranking of arrayed ligand-analyte interactions. *Anal. Biochem.* **500**, 21–23 (2016).
 45. Tiwari, P. B., Wang, X., He, J. & Darici, Y. Analyzing surface plasmon resonance data: Choosing a correct biphasic model for interpretation. *Rev. Sci. Instrum.* **86**, 1–9 (2015).
 46. Fischer, J., Dickhut, A., Rickert, M. & Richter, W. Human articular chondrocytes secrete parathyroid hormone-related protein and inhibit hypertrophy of mesenchymal stem cells in coculture during chondrogenesis. *Arthritis Rheum.* **62**, 2696–2706 (2010).
 47. Korchynskyi, O. & Ten Dijke, P. Identification and functional characterization of distinct critically important bone morphogenetic protein-specific response elements in the Id1 promoter. *J. Biol. Chem.* **277**, 4883–4891 (2002).
 48. Promega. Quantifluor dye systems data analysis workbook. Available at: www.promega.com/resources/tools/quantifluor-dye-systems-data-analysis-workbook/.
 49. MN. NucleoSpin® RNA Plus RNA isolation User manual. Available at: <https://www.mn-net.com/media/pdf/83/75/16/Instruction-NucleoSpin-RNA-Plus.pdf>.
 50. Pierce. User Guide: Pierce BCA Protein Assay Kit. Available at: https://assets.thermofisher.com/TFS-Assets/LSG/manuals/MAN0011430_Pierce_BCA_Protein_Asy_UG.pdf.
 51. NCBI protein blast. Available at: <https://blast.ncbi.nlm.nih.gov/Blast.cgi>.

52. Geiger, B. & Yamada, K. M. Molecular architecture and function of matrix adhesions. *Cold Spring Harb. Perspect. Biol.* **3**, 1–21 (2011).
53. Zilberberg, L., ten Dijke, P., Sakai, L. Y. & Rifkin, D. B. A rapid and sensitive bioassay to measure bone morphogenetic protein activity. *BMC Cell Biol.* **8**, 1–10 (2007).
54. Shen, B. *et al.* The role of BMP-7 in chondrogenic and osteogenic differentiation of human bone marrow multipotent mesenchymal stromal cells in vitro. *J. Cell. Biochem.* **109**, 406–416 (2010).
55. Tuli, R. *et al.* Transforming Growth Factor- β -mediated Chondrogenesis of Human Mesenchymal Progenitor Cells Involves N-cadherin and Mitogen-activated Protein Kinase and Wnt Signaling Cross-talk. *J. Biol. Chem.* **278**, 41227–41236 (2003).
56. Schasfoort, R. B. M. *Handbook of Surface Plasmon Resonance. Handbook of Surface Plasmon Resonance* (2017). doi:10.1039/9781788010283
57. Khodr, V., Machillot, P., Migliorine, E., Reiser, J.-B. & Picart, C. High throughput measurements of BMP/BMP receptors interactions using bio-layer interferometry. *bioRxiv* 1–24 (2020).
58. Chen, X., Zaro, J. & Shen, W.-C. Fusion Protein Linkers: Property, Design and Functionality. *Adv Drug Deliv Rev.* **65**, 1–32 (2013).
59. Beirnaert, E. *et al.* Bivalent llama single-domain antibody fragments against tumor necrosis factor have picomolar potencies due to intramolecular interactions. *Front. Immunol.* **8**, (2017).
60. Katsumi, A., Orr, A. W., Tzima, E. & Schwartz, M. A. Integrins in Mechanotransduction. *J. Biol. Chem.* **279**, 12001–12004 (2004).
61. Sun, Z., Guo, S. S. & Fässler, R. Integrin-mediated mechanotransduction. **215**, (2016).
62. Liang, W. *et al.* Periodic mechanical stress INDUCES chondrocyte proliferation and matrix synthesis via CaMKII-mediated Pyk2 signaling. *Cell. Physiol. Biochem.* **42**, 383–396 (2017).
63. Riss, T. L. *et al.* *Cell Viability Assays. Promega Corporation* (2016).
64. Loeser, R. F., Sadiev, S., Tan, L. & Goldring, M. B. Integrin expression by primary and immortalized human chondrocytes: Evidence of a differential role for $\alpha 1\beta 1$ and $\alpha 2\beta 1$ integrins in mediating chondrocyte adhesion to types II and VI collagen. *Osteoarthr. Cartil.* **8**, 96–105 (2000).
65. Chubinskaya, S. *et al.* Regulation of chondrocyte gene expression by osteogenic protein-1. *Arthritis Res. Ther.* **13**, 1–14 (2011).
66. Huang, X., Zhong, L., Post, J. N. & Karperien, M. Co-treatment of TGF- $\beta 3$ and BMP7 is superior in stimulating chondrocyte redifferentiation in both hypoxia and normoxia compared to single treatments. *Sci. Rep.* **8**, 1–10 (2018).
67. Ripmeester, E. G. J., Timur, U. T., Caron, M. M. J. & Welting, T. J. M. Recent insights into the contribution of the changing hypertrophic chondrocyte phenotype in the development and progression of osteoarthritis. *Front. Bioeng. Biotechnol.* **6**, (2018).
68. Nguyen, C. *et al.* Revisiting spatial distribution and biochemical composition of calcium-containing crystals in human osteoarthritic articular cartilage. *Arthritis Res. Ther.* **15**,

- (2013).
69. Zaucke, F. Cartilage Glycoproteins. *Cartil. Physiol. Dev.* **1**, 55–81 (2016).
 70. Rafael, M. S. *et al.* Insights into the association of Gla-rich protein and osteoarthritis, novel splice variants and γ -carboxylation status. *Mol. Nutr. Food Res.* **58**, 1636–1646 (2014).
 71. Posey, K. & Hecht, J. The Role of Cartilage Oligomeric Matrix Protein (COMP) in Skeletal Disease. *Curr. Drug Targets* **9**, 869–877 (2008).
 72. Heinegård, D. & Saxne, T. The role of the cartilage matrix in osteoarthritis. *Nat. Rev. Rheumatol.* **7**, 50–56 (2011).
 73. Lozito, T. P. *et al.* Three-dimensional osteochondral microtissue to model pathogenesis of osteoarthritis. **4**, 1–6 (2013).
 74. Zhong, L., Huang, X., Karperien, M. & Post, J. N. Correlation between gene expression and osteoarthritis progression in human. *Int. J. Mol. Sci.* **17**, 1–14 (2016).
 75. Ströbel, S. *et al.* Anabolic and catabolic responses of human articular chondrocytes to varying oxygen percentages. *Arthritis Res. Ther.* **12**, 1–15 (2010).

8. Supplementary data

List of primers used in qPCR

Table S1: Sequence, T_m and MW/bp of the primers used for qPCR

Oligo name	Sequence (5'-3')	MW	T _m °	bp
Hum ID1_1 for	AGAACCGCAAGGTGAGCAA	5880	65.9	
Hum ID1_1 rev	TCCAAGTGAAGGTCCCTGATG	6406	66.3	
Hum ID1_2 for	CTGCTCTACGACATGAACGG	6102	63.5	
Hum ID1_2 rev	GAAGGTCCCTGATGTAGTCGAT	6790	63.1	
Human Sox9 for	TGGGCAAGCTCTGGAGACTTC		60	98
Human Sox9 rev	ATCCGGGTGGTCCTTCTTGTC		60	
Hum Runx2 for	GGAGTGGACGAGGCCAAGAGTTT		60	133
Hum Runx2 rev	AGCTTCTGTCTGTGCCTTCTGG		60	
Hum TCF1 for	AGGAGTGCAATAGGGCGGAATG		60	133
Hum TCF1 rev	CCGGTTGGCAAACCAAGTTGTAG		60	
Hum LEF1 for	CGAAGAGGAAGGCGATTTAG		60	109
Hum LEF1 rev	CTGAGAGGTTTGTGCTTGTC		60	
Hum B2M for	GACTTGTCTTTTCAGCAAGGA		60	106
Hum B2M rev	ACAAAGTCACATGGTTCACA		60	

Macro for measuring circularity in ImageJ

Open all images

plugins, macros, edit

Click run, wait, repeat until all images are analyzed and closed

```
T = getTitle();
run("Split Channels");
selectWindow("C1-"+T);
run("8-bit")
run("8-bit")
titleBlue = getTitle;
close();

selectWindow("C2-"+T);
run("8-bit")
run("8-bit")
titleGreen = getTitle;
setThreshold(24, 255);
setOption("BlackBackground", false);
run("Convert to Mask");
run("Analyze Particles...", "size=90-Infinity show=Outlines display clear include");
run("Summarize");
selectWindow("Results");
saveAs("Measurements", T+"Results.csv");
close();
close()
selectWindow("Results");
run("Close");
```


Macro to create a montage of fluorescent images in ImageJ (DAPI, Phalloidin and anti-VHH staining)

```
T = getTitle();
run("Split Channels");
selectWindow("C1-"+T);
run("8-bit")
run("8-bit")
titleBlue = getTitle;

selectWindow("C2-"+T);
run("8-bit")
run("8-bit")
titleGreen = getTitle;

selectWindow("C3-"+T);
run("8-bit")
run("8-bit")
titleRed = getTitle;

run("Merge Channels...", "c1="+titleRed+" c2="+titleGreen+" c3="+titleBlue+" ");
run("Scale Bar...", "width=10 height=4 font=14 color=White background=None location=[Lower Right] bold overlay");
run("RGB to Montage", "rows=horizontal border=3 scale=10 colourisation=Greys");
saveAs("Tiff", "folder name \\"+T+" montage");
close();
selectWindow("RGB");
close();
```

SPRI data obtained using Matlab file

Table S2: kon, koff and KD determined by double fit, non-fixed method with ITGB1 analyte concentrations of 256, 128 and 64 nM.

	k _{on}	k _{off}	KD	Fitting
BMP-ITGB1-3C9a256nM	k _{on} 1: 2.164 e5 k _{on} 2: 6.790 e3	k _{off} 1: 4.274 e-3 k _{off} 2: 4.775 e-4	KD1: 1.975 e-08 KD2: 7.032 e-08 WeightedKD: 19.77 nM	
BMP-ITGB1-3C9a128nM	k _{on} 1: 2.424 e5 k _{on} 2: 7.799 e3	k _{off} 1: 9.078 e-3 k _{off} 2: 4.332 e-3	KD1: 3.746 e-08 KD2: 5.554 e-07 WeightedKD: 37.79 nM	
BMP-ITGB1-3C9a64nM	k _{on} 1: 1.000 e6 k _{on} 2: 1.656 e4	k _{off} 1: 1.000 e-6 k _{off} 2: 4.458 e-3	KD1: 1.000 e-12 KD2: 2.686 e-07 WeightedKD: 0.01188 nM	
BMP-ITGB1-14F8a256nM	k _{on} 1: 7.407 e4 k _{on} 2: 4.147 e3	k _{off} 1: 2.446 e-3 k _{off} 2: 1.657 e-5	KD1: 3.302 e-08 KD2: 3.995 e-09 WeightedKD: 32.95 nM	

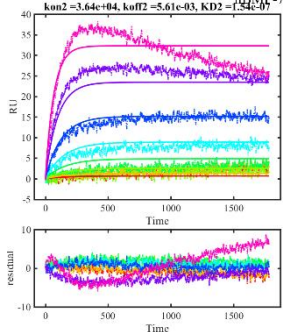
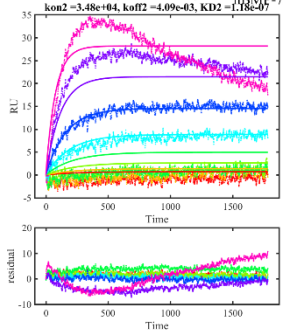
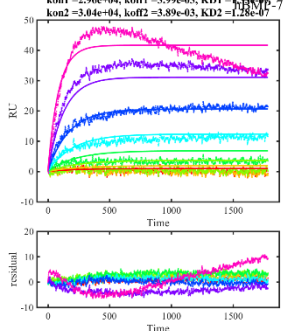
BMP-ITGB1-14F8a128nM	k_{on1} : 1.567 e5 k_{on2} : 5.316 e3	k_{off1} : 2.300 e-3 k_{off2} : 1.000 e-6	KD1: 1.468 e-08 KD2: 1.881 e-10 WeightedKD: 14.67 nM	<p>$k_{on1} = 1.57e+05, k_{off1} = 2.30e-03, KD1 = 1.47e-08$ $k_{on2} = 5.32e+03, k_{off2} = 1.00e-06, KD2 = 1.88e-10$</p>
BMP-ITGB1-14F864nM	k_{on1} : 3.061 e5 k_{on2} : 8.087 e3	k_{off1} : 3.439 e-3 k_{off2} : 1.000 e-6	KD1: 1.124 e-08 KD2: 1.237 e-10 WeightedKD: 11.23 nM	<p>$k_{on1} = 3.06e+05, k_{off1} = 3.44e-03, KD1 = 1.12e-08$ $k_{on2} = 8.09e+03, k_{off2} = 1.00e-06, KD2 = 1.24e-10$</p>
BMP7-G7a256nM	k_{on1} : 4.658 e3 k_{on2} : 4.658 e3	k_{off1} : 1.000 e-6 k_{off2} : 1.000 e-6	KD1: 2.147e-10 KD2: 2.147e-10 WeightedKD: 0.2147 nM	<p>$k_{on1} = 4.66e+03, k_{off1} = 1.00e-06, KD1 = 2.15e-10$ $k_{on2} = 4.66e+03, k_{off2} = 1.00e-06, KD2 = 2.15e-10$</p>
BMP7-G7a128nM	k_{on1} : 1.000 e4 k_{on2} : 2.500 e3	k_{off1} : 1.000 e-4 k_{off2} : 2.500 e-5	KD1: 1e-08 KD2: 1e-08 WeightedKD: 10 nM	<p>$k_{on1} = 1.00e+04, k_{off1} = 1.00e-04, KD1 = 1.00e-08$ $k_{on2} = 2.50e+03, k_{off2} = 2.50e-05, KD2 = 1.00e-08$</p>
BMP7-G7a64nM	k_{on1} : 1.000 e4 k_{on2} : 2.500 e3	k_{off1} : 1.000 e-4 k_{off2} : 2.500 e-5	KD1: 1e-08 KD2: 1e-08 WeightedKD: 10 nM	<p>$k_{on1} = 1.00e+04, k_{off1} = 1.00e-04, KD1 = 1.00e-08$ $k_{on2} = 2.50e+03, k_{off2} = 2.50e-05, KD2 = 1.00e-08$</p>

BSAa64nM	k_{on1} : 1.000 e4 k_{on2} : 2.500 e3	k_{off1} : 1.000 e-4 k_{off2} : 2.500 e-5	KD1: 1e-08 KD2: 1e-08 WeightedKD: 10 nM	
BSAa128nM	k_{on1} : 1.000 e4 k_{on2} : 2.500 e3	k_{off1} : 1.000 e-4 k_{off2} : 2.500 e-5	KD1: 1e-08 KD2: 1e-08 WeightedKD: 10 nM	
BSAa256nM	k_{on1} : 1.000 e4 k_{on2} : 2.500 e3	k_{off1} : 1.000 e-4 k_{off2} : 2.500 e-5	KD1: 1e-08 KD2: 1e-08 WeightedKD: 10 nM	

Table S3: k_{on} , k_{off} and KD determined by double fit, non-fixed method with BMP-7 analyte concentrations of 256, 128 and 64 nM.

	K_{on}	K_{off}	KD	Fitting
BMP-ITGB1-3C9a256nM	k_{on1} : 5.806 e4 k_{on2} : 2.572 e3	k_{off1} : 5.644 e-3 k_{off2} : 1.336 e-3	$KD1$: 9.720 e-08 $KD2$: 5.195 e-07 WeightedKD: 98.88 nM	<p>$k_{on1} = 5.81e+04$, $k_{off1} = 5.64e-03$, $KD1 = 9.72e-08$ $k_{on2} = 2.57e+03$, $k_{off2} = 1.34e-03$, $KD2 = 5.19e-07$ - hBMP-7256 2</p>
BMP-ITGB1-3C9a128nM	k_{on1} : 2.581 e3 k_{on2} : 1.154 e3	k_{off1} : 2.388 e-3 k_{off2} : 6.831 e-4	$KD1$: 9.253 e-07 $KD2$: 5.920 e-07 WeightedKD: 914.60 nM	<p>$k_{on1} = 2.58e+03$, $k_{off1} = 2.39e-03$, $KD1 = 9.25e-07$ $k_{on2} = 1.15e+03$, $k_{off2} = 6.83e-04$, $KD2 = 5.92e-07$ - hBMP-7256 2</p>
BMP-ITGB1-3C9a64nM	k_{on1} : 3.622 e4 k_{on2} : 1.827 e3	k_{off1} : 6.609 e-3 k_{off2} : 1.170 e-3	$KD1$: 1.825 e-07 $KD2$: 6.402 e-07 WeightedKD: 184 nM	<p>$k_{on1} = 3.62e+04$, $k_{off1} = 6.61e-03$, $KD1 = 1.82e-07$ $k_{on2} = 1.83e+03$, $k_{off2} = 1.17e-03$, $KD2 = 6.40e-07$ - hBMP-7256 2</p>
BMP-ITGB1-14F8a256nM	k_{on1} : 2.990 e4 k_{on2} : 1.401 e3	k_{off1} : 1.585 e-3 k_{off2} : 7.145 e-4	$KD1$: 5.302 e-08 $KD2$: 5.099 e-07 WeightedKD: 57.78 nM	<p>$k_{on1} = 2.99e+04$, $k_{off1} = 1.59e-03$, $KD1 = 5.30e-08$ $k_{on2} = 1.40e+03$, $k_{off2} = 7.14e-04$, $KD2 = 5.10e-07$ - hBMP-7256 2</p>

BMP-ITGB1-14F8a128nM	k_{on1} : 6.862 e4 k_{on2} : 2.990 e3	k_{off1} : 3.030 e-3 k_{off2} : 1.430 e-3	KD1: 4.416 e-08 KD2: 4.783 e-07 WeightedKD: 46.28 nM	$k_{on1} = 6.86e+04, k_{off1} = 3.03e-03, KD1 = 4.416e-08$ $k_{on2} = 2.99e+03, k_{off2} = 1.43e-03, KD2 = 4.78e-07$
BMP-ITGB1-14F864nM	k_{on1} : 5.974 e4 k_{on2} : 2.891 e3	k_{off1} : 4.379 e-3 k_{off2} : 1.363 e-3	KD1: 7.329 e-08 KD2: 4.715 e-07 WeightedKD: 75.24 nM	$k_{on1} = 5.97e+04, k_{off1} = 4.38e-03, KD1 = 7.329e-08$ $k_{on2} = 2.89e+03, k_{off2} = 1.36e-03, KD2 = 4.71e-07$
BMP7-G7a256nM	k_{on1} : 1.022 e4 k_{on2} : 3.316 e3	k_{off1} : 2.606 e-3 k_{off2} : 1.019 e-8	KD1: 2.550 e-07 KD2: 3.074 e-12 WeightedKD: 254.4 nM	$k_{on1} = 1.02e+04, k_{off1} = 2.61e-03, KD1 = 2.55e-07$ $k_{on2} = 3.32e+03, k_{off2} = 1.02e-08, KD2 = 3.07e-12$
BMP7-G7a128nM	k_{on1} : 4.799 e4 k_{on2} : 2.144 e3	k_{off1} : 4.691 e-3 k_{off2} : 1.059 e-3	KD1: 9.776 e-08 KD2: 4.940 e-07 WeightedKD: 99.24 nM	$k_{on1} = 4.80e+04, k_{off1} = 4.69e-03, KD1 = 9.776e-08$ $k_{on2} = 2.14e+03, k_{off2} = 1.06e-03, KD2 = 4.94e-07$
BMP7-G7a64nM	k_{on1} : 4.175 e4 k_{on2} : 2.022 e3	k_{off1} : 2.189 e-3 k_{off2} : 3.984 e-4	KD1: 5.244 e-08 KD2: 1.970 e-07 WeightedKD: 52.62 nM	$k_{on1} = 4.17e+04, k_{off1} = 2.19e-03, KD1 = 5.244e-08$ $k_{on2} = 2.02e+03, k_{off2} = 3.98e-04, KD2 = 1.97e-07$

BSAa64nM	k_{on1} : 3.644 e4 k_{on2} : 3.640 e4	k_{off1} : 5.683 e-3 k_{off2} : 5.612 e-3	$KD1$: 1.560 e-07 $KD2$: 1.542 e-07 WeightedKD: 1.560 e-07	<p>kon1 = 3.64e+04, koff1 = 5.68e-03, KD1 = 1.56e-07 kon2 = 3.64e+04, koff2 = 5.61e-03, KD2 = 1.54e-07</p> 
BSAa128nM	k_{on1} : 3.501 e4 k_{on2} : 3.479 e4	k_{off1} : 4.058 e-3 k_{off2} : 4.089 e-3	$KD1$: 1.159 e-07 $KD2$: 1.175 e-07 WeightedKD: 1.159 e-07	<p>kon1 = 3.50e+04, koff1 = 4.06e-03, KD1 = 1.16e-07 kon2 = 3.48e+04, koff2 = 4.09e-03, KD2 = 1.18e-07</p> 
BSAa256nM	k_{on1} : 2.963 e4 k_{on2} : 3.038 e4	k_{off1} : 3.985 e-3 k_{off2} : 3.893 e-3	$KD1$: 1.345 e-07 $KD2$: 1.281 e-07 WeightedKD: 1.345 e-07	<p>kon1 = 2.96e+04, koff1 = 3.99e-03, KD1 = 1.35e-07 kon2 = 3.04e+04, koff2 = 3.89e-03, KD2 = 1.28e-07</p> 

Optimization luciferase assay for BMP-7

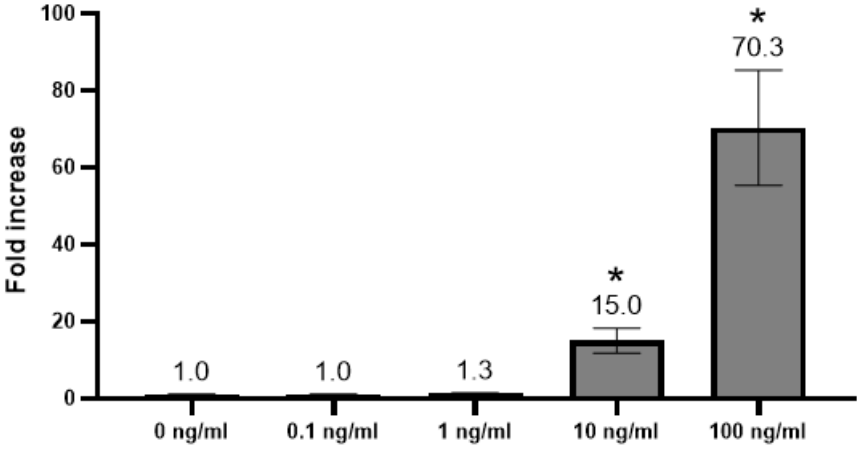
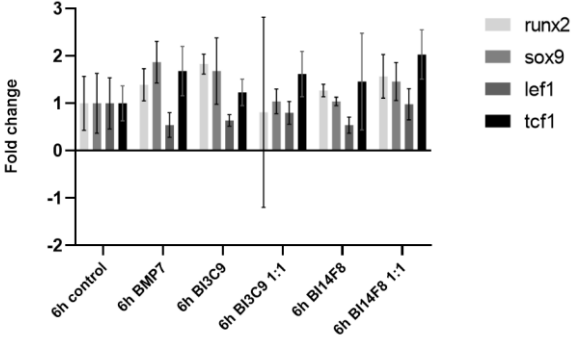


Figure S1: Relative BRE-Luc expression after 14 hours of stimulating C2C12 BRE-Luc cells with different concentrations of BMP-7 (Mean ± 95%-CI). Data was expressed as fold change compared to the control. * p < 0.05 compared to the negative control 0 ng/ml.

qPCR results

6h



24h

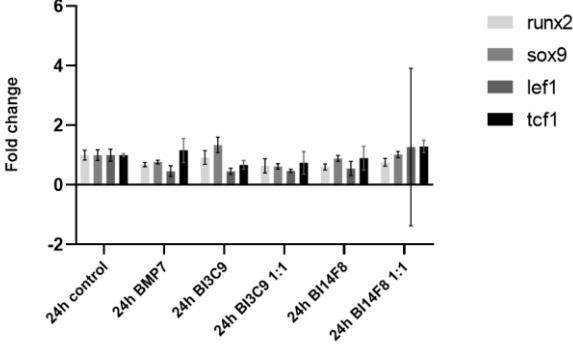


Figure S2: qPCR result of the genes Runx2, Sox9, Lef1 and Tcf1. The results were insignificant compared to the negative control and free BMP-7.

Table S4: Intensity of the detected bands, measured as percentage of the four analyzed bands. The detected antibodies are p-Smad1/5/8, Smad1/5/8 and beta actin.

Detected antibody	Stimulation time (min)	Membrane 1	Membrane 2
p-Smad1/5/8	15	25.580	20.539
	30	33.513	28.004
	60	21.248	28.957
	120	19.659	22.500
Smad1/5/8	15	20.074	25.407
	30	32.252	25.843
	60	24.115	21.912
	120	23.559	26.839
Beta actin	15	24.140	24.933
	30	25.812	28.055
	60	22.955	21.936
	120	27.094	25.075